Aus dem NeuroCure Clinical Research Center
und dem Institut für Neuroradiologie
der Medizinischen Fakultät Charité – Universitätsmedizin Berlin

DISSERTATION

Evaluation of Optic Pathway Degeneration via Optic Chiasm
Assessment in Conventional Magnetic Resonance Imaging

Beurteilung der Degeneration der optischen Bahn via Chiasma
Opticum Messung in der konventionellen
Magnetresonanztomographie

zur Erlangung des akademischen Grades
Doctor medicinae (Dr. med.)

vorgelegt der Medizinischen Fakultät
Charité – Universitätsmedizin Berlin

von

Valentin Jünger

aus Rosenheim

Datum der Promotion: 04.03.2022

Table of Contents

<u>List of Abbreviations</u>

AUC	Area under the curve
AQP4-IgG	aquaporin 4-IgG
CI	95% Confidence Interval
CoV	coefficient of variation
EDSS	Expanded Disability Status Scale
FLAIR	fluid-attenuated inversion recovery sequence
GCIPL	combined ganglion cell-inner plexiform layer
HC	healthy controls
logMAR	logarithm of the minimum angle of resolution
ICC	intraclass correlations
MPRAGE	Magnetization Prepared Rapid Gradient Echo
MRI	magnetic resonance imaging
NMOSD	neuromyelitis optica spectrum disorders
NMOSD-ON	neuromyelitis optica patients with history of optic neuritis
NMOSD-NON	neuromyelitis optica patients without history of optic neuritis
OCT	optical coherence tomography
pRNFL	peripapillary retinal nerve fiber layer
ROC	Receiver Operating Characteristics

Synopsis

Abstract (English)

Background:

The optic pathway is preferentially targeted by inflammatory central nervous system diseases such as neuromyelitis spectrum disorders (NMOSD). The neurodegenerative damage that follows an optic neuritis may involve the entire visual pathway. Currently there is no validated method available to evaluate this damage on conventional MRI. Axons from both optic nerves merge at the optic chiasm, making it a promising imaging marker of neurodegenerative changes of the anterior optic pathway.

Objectives:

The aim of this dissertation project was to investigate whether neurodegenerative changes of the anterior optic pathway can be detected by measuring optic chiasm dimensions. Therefore, we hypothesized that neurodegenerative changes of the anterior optic pathway manifest in a reduction of optic chiasm dimensions and that optic chiasm dimensions in conventional 3D T1-weighted MR images are sensitive to neurodegenerative changes of anterior optic pathway.

Materials and Methods:

In a cross-sectional study, we used NMOSD as a model of severe optic pathway damage and measured optic chiasm dimensions of 39 aquaporin 4-IgG-seropositive NMOSD patients, of which 25 had a history of optic neuritis (NMOSD-ON), and 37 age- and sex- matched healthy control participants. To test our hypothesis optic chiasm dimensions between patients and healthy control participants were compared. The sensitivity with which these predict the presence of damage of the anterior optic pathway was assessed in a receiver operating characteristics analysis. Additional associations with structural measures of the anterior optic pathway (optic nerve atrophy in MRI, retinal ganglion cell loss in optical coherence tomography

(OCT)) and clinical parameters (visual acuity as logarithm of the minimum angle of resolution (logMAR) and disease duration) were analyzed.

Results:

Compared to healthy control participants optic chiasm height and area were smaller in NMOSD-ON patients (p<0.0001) and NMOSD-NON patients (p<0.01). An optic chiasm area smaller than 22.5 mm^2 yielded a sensitivity of 0.92 and a specificity of 0.92 in differentiating the optic chiasm of NMOSD-ON from healthy control participants. The optic chiasm area correlated with structural measures of the anterior optic pathway in NMOSD-ON, i.e. optic nerve diameter (r=0.4, p=0.047), peripapillary retinal nerve fiber layer thickness (r=0.59, p=0.003)) and clinical parameters, e.g. visual acuity (r=-0.57, p=0.013) and disease duration (r=-0.5, p=0.012).

Conclusion:

Optic chiasms are significantly smaller in NMOSD patients compared to healthy control patients. The optic chiasm area, as measured with conventional MRI, is associated with structural measures of the anterior optic pathway and clinical parameters. Our results suggest that optic chiasm dimensions are promising and easily accessible imaging markers for the assessment of neurodegenerative changes of the anterior optic pathway.

Abstract (German)

Hintergrund:

Das visuelle System ist in neuroinflammatorischen Erkrankungen wie Neuromyelitis optica häufig betroffen. Neurodegenerativer Schaden nach Optikusneuritis kann die gesamte optische Bahn betreffen. Aktuell gibt es keine validierte Methode zur Beurteilung neurodegenerativen Schadens der anterioren optischen Bahn auf Routine-MRT Aufnahmen. Axone beider Nervi optici laufen im Chiasma opticum zusammen, was es zu einem vielversprechenden Bildgebungsmarker neurodegenerativer Veränderungen der anterioren optischen Bahn macht.

Ziel:

Ziel war es zu untersuchen, ob neurodegenerative Veränderungen der anterioren optischen Bahn am Chiasma opticum sensitiv und zuverlässig detektierbar sind. Unsere Hypothese ist, dass sich neurodegenerative Veränderungen der anterioren optischen Bahn durch Atrophie des Chiasma opticums manifestieren und, dass Größenparameter des Chiasma opticums in konventionellen 3D T1-gewichteten MRT Aufnahmen sensitiv gegenüber dieser Veränderungen sind.

Methoden:

In einer Querschnittsstudie wurden Patienten mit NMOSD als Modell für schweren Schaden der anterioren optischen Bahn untersucht. Die Größenparamenter Höhe, Breite, Fläche des Chiasma opticums von 39 Aquaporin-4-IgG seropositiven NMOSD Patienten (davon 25 mit Optikusneuritis Anamnese) und 37 in Alter und Geschlecht gematchte, gesunde Kontrollprobanden wurden bestimmt und verglichen. Sensitivität und Spezifität, mit der diese Parameter Schaden der anterioren optischen Bahn nachweisen, wurden in einer Receiver Operating Characteristics Analyse untersucht. Es wurden Assoziationen mit strukturellen Parametern der anterioren optischen Bahn (Nervus opticus Atrophie im MRT, Verlust retinaler

Ganglionzellen im OCT) und klinischen Parametern (Sehschärfe als logMAR, Krankheitsdauer) analysiert.

Ergebnisse:

Verglichen mit Kontrollprobanden waren Höhe und Fläche des Chiasma opticums signifikant kleiner in NMOSD-Patienten, sowohl bei Patienten mit Optikusneuritis Anamnese (NMOSD-ON $p<0.0001$) als auch ohne (NMOSD-NON $p<0.01$). Eine Chiasma opticum Fläche von kleiner als $22.5mm^2$ trennte NMOSD-ON Patienten von Kontrollprobanden mit einer Sensitivität von 0.92 und einer Spezifität von 0.92. Die Chiasma opticum Fläche korrelierte mit strukturellen Maßen der anterioren optischen Bahn in NMOSD-ON Patienten, z.B. Nervus opticus Durchmesser ($r=0.4$, $p=0.047$), pRNFL Dicke ($r=0.59$, $p=0.003$), und mit klinischen Parametern, wie der Sehschärfe ($r=-0.57$, $p=0.013$) und der Krankheitsdauer ($r=-0.5$, $p=0.012$)).

Schlussfolgerung:

Zwischen NMOSD-Patienten und Kontrollprobanden bestehen deutliche Größenunterschiede des Chiasma opticums. Diese sind mit strukturellen Maßen der anterioren optischen Bahn und klinischen Parametern assoziiert. Unsere Ergebnisse zeigen, dass die Größenparameter des Chiasma opticums vielversprechende und einfach zugängliche Bildgebungsmarker für die Beurteilung neurodegenerativer Veränderungen der anterioren optischen Bahn sind.

Introduction

As visual animals, humans depend on their sense of sight. The optic pathway transmits visual information collected at the retina via the optic chiasm to the visual cortex. Inflammatory autoimmune central nervous system diseases, such as neuromyelitis optic spectrum disorders (NMOSD), frequently target the optic pathway, causing acute attacks of inflammation and long term degeneration. Clinical outcomes are impaired visual function and reduction of vision-related quality of life. Early detection of optic pathway degeneration is crucial for on-time intervention and preservation of vision. This study examined whether optic chiasm measures are useful markers of anterior optic pathway degeneration in NMOSD. It was conducted as a doctorate by publication and partial results have been published. (1)

The optic pathway

The optic pathway transmits signals from the eye to the brain via four anatomical structures: First the retina, second the optic nerves, the optic chiasm and the optic tracts, third the lateral geniculate body and the optic radiation and fourth the visual cortex. The different anatomical structures are schematically illustrated in Figure 1 and consist of four neuronal structures. By means of the first neuronal structure, the photoreceptors located in the retina, light rays are converted to electrochemical signals. These are processed by bipolar interneurons, the second neuronal structure and passed on to the retinal ganglion cells, the third neuronal structure. The different types of neurons in the retina form the retinal layers. Figure 2A schematically illustrates the anatomy of the retina and the assembling of its layers. The peripapillary retinal nerve fiber layer (pRNFL) consists of unmyelinated axons of retinal ganglion cells which lead toward the optic disc and out of the eye, where they pass on as the myelinated optic nerve. The axons from the left and the right optic nerve merge in the optic chiasm partly traversing to the contralateral side, pass on as the optic tract and terminate in the lateral geniculate body of the thalamus. The lateral geniculate body represents the boundary between the anterior and the

posterior optic pathway. Axons of the optic tract build synapses with the fourth neuronal structure, the neurons of the optic radiation. These end in the visual cortex, specifically Brodmann's area 17, where the visual signals are further processed. Instead of synapsing in the thalamus, some retinal ganglion axons terminate in the pretectal portion of the midbrain, forming the afferent arm of the pupillary light reflex. (2)
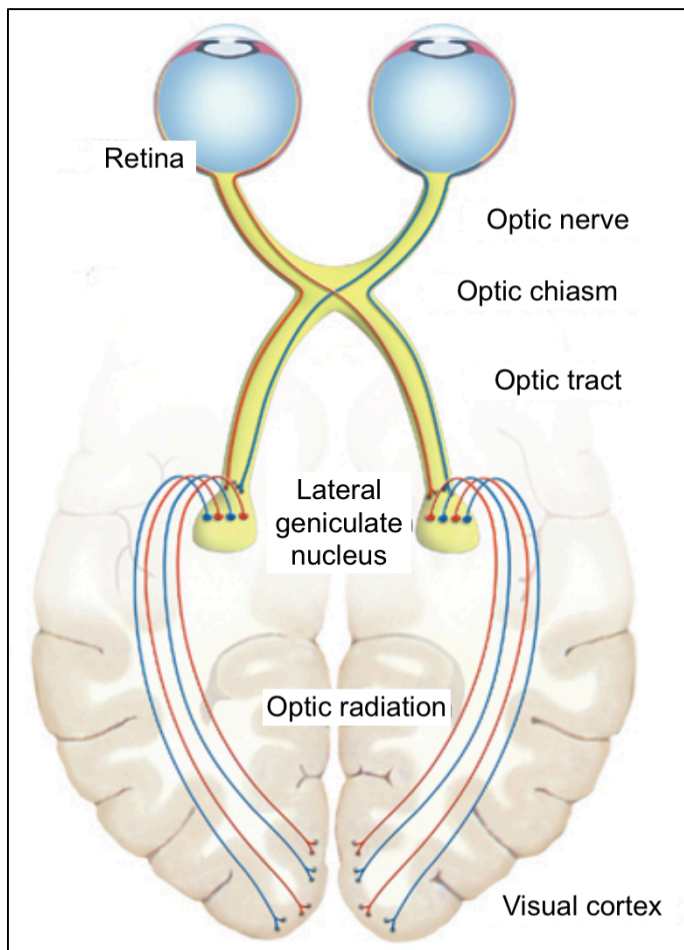

Figure 1: Schematic view of the visual pathway.

The optic chiasm accumulates axons from both sides anteriorly connected to the retina, forming the optic nerves and posteriorly passing on to the optic tracts. Adapted from Zimmermann 2017

(3)

Optic pathway degeneration

Optic pathway degeneration in inflammatory autoimmune central nervous system diseases results from damage to the nerve fibers following inflammation. Damaged nerve fibers are restricted in their function to transmit electrical signals from the retina to the visual cortex. As a consequence, visual function may reduce to varying degrees.

Optic neuritis, or inflammation of the optic nerve, is a common clinical presentation in NMOSD that are frequently associated with serum autoantibodies to aquaporin-4. (4) It is characterized by retrobulbar pain on eye movement, a decrease in visual acuity and long term visual impairment. (5) Optic pathway degeneration following optic neuritis includes anterograde and retrograde trans-synaptic degeneration (6–8) and results in atrophy involving the entire optic pathway from the retina, along the optic nerves and anatomically connected tracts to the visual cortex. (9,10) Atrophy comprises axonal loss and demyelination, which may also contribute to the underlying pathophysiology, hereby causing a reduction in the size of the affected structure. The optic chiasm, as the site where nerve fibers accumulate, is crucial in this context. As illustrated in Figure 1, fibers from the left and right optic nerve merge at the optic chiasm and form a site of high axonal density. It, therefore, captures all fibers anteriorly originating in the retina and posteriorly passing on as the optic tracts. Direct damage or other pathophysiological effects affecting the optic pathway may accumulate in the optic chiasm, making it a promising target for the assessment of anterior optic pathway damage. Early detection of optic pathway degeneration is vital for timely intervention and preservation of vision, since currently no therapy to reverse neurodegenerative damage of the optic pathway is available. (11)

Measures of optic pathway degeneration

Measures of optic pathway degeneration are related to impaired visual function and reduction of vision-related quality of life and therefore are an important outcome measure of optic neuritis. (5,11) MRI measures are used to evaluate degeneration of the optic pathway from the

optic nerves to the visual cortex. Although MRI is broadly available as part of the routine clinical work-up of NMOSD patients (12), no standardized method to evaluate optic pathway degeneration in conventional MRI has been established.

The underlying physical principle of MRI is nuclear magnetic resonance. Strong magnetic fields generated by the MRI scanner cause the atoms in the different tissues to arrange their proton spins in alignment with the external magnetic field. This state is called the equilibrium state. During a processes called excitation, radio wave pulses trigger protons in the equilibrium state to fall out of the alignment. Relaxation describes the process after withdrawing the excitatory radio wave pulse. The protons return to the equilibrium state and emit a radio frequency signal. This signal is determined by the degree of excitation and the time in which excited atoms return to the alignment within the magnetic field. Since this rate depends on the tissue the atoms reside in, the signal can be used to determine the contrast between different tissues. (13) Two independent relaxation processes are important in conventional MRI. T1 describes the spin-lattice relaxation, that is the relaxation parallel to the applied magnetic field and T2 describes the spin-spin relaxation, that is the relaxation transverse to the applied magnetic field. Weighting images by the relaxation processes can be useful to maximize contrast of specific tissues. For instance T1-weighted images have low signal intensities from CSF, while standard T2-weighted images have high signal intensities from CSF. (13)

In MRI, optic pathway dimensions have been used as surrogate markers of inflammatory damage and atrophy of the optic nerve and anatomically connected tracts and their reductions have been quantified to estimate the extent of neurodegenerative damage. (14–20) Optic pathway assessment derived from measurements at all levels of the optic pathway, including the optic nerves, the optic chiasm, the optic tracts, the lateral geniculate body and the visual cortex have been proposed. (9,10,17–22) The most prominent methods focus on the assessment of the optic nerve. One major problem in optic nerve assessment is the definition of standardized measurement locations along the variable course of the nerve. While some studies suggest optic

nerve assessment at the retro-orbital portion (18), others refer to the intra-orbital portion. Even studies referring to the intra-orbital portion split in those including (17), and those excluding the retrobulbar portion (14). Furthermore, their definition of measurement locations is not uniform: They are defined either by a distance from the orbital apex (14), or a distance from the retina (23) or by the slice in which the optic nerve appears most round (24). This is problematic, because not only the length of the optic nerve, but also its diameter vary between different portions and subjects. (2,17) Additionally, the measurement accuracy of MRI along the optic nerve varies, since each part presents different challenges. In the anterior part, motion artefacts from eye movements render accurate assessment difficult. The posterior region is characterized by thinning of its surrounding CSF-filled sub-arachnoid space as the nerve proceeds towards the optic chiasm, which results in reduced contrast for an accurate nerve assessment. (17) The difficulty in accurately measuring the optic nerve arising from the anatomical variability and the varying measurement accuracy is reflected in the high inter-individual variability in its measures even in the healthy population. (14–17,19)

Technically, optic nerve imaging typically involves dedicated orbital MRI fat-saturated acquisition sequences along the axis of the optic nerve (14–16,19) in addition to the commonly acquired sequences and this extends the scan time for each patient. Others involve complex imaging post-processing procedures (17) and, thus, may be difficult to implement in the routine clinical work-up. Recent studies suggest volumetric approaches but these are so far not applicable to clinical standard of care imaging protocols (17) or require time-consuming manual segmentation. (20)

Optical coherence tomography (OCT) is a medical imaging technique that creates scans of the retina through low coherence interferometry. OCT measures are used to evaluate retinal degeneration. The OCT devices emit continuous near-infrared light waves that travel through the pupil and get reflected by retinal structures. On the basis of the properties of the reflected light waves, retinal scans are generated. Analogous to ultrasonography, the major underlying

physical principles determining image contrast are absorption, back scatter and time delay. While absorption and back-scatter are defined by the optical characteristics of the specific anatomical structures, time delay of the echoes depend on the depth of the structure, that is the distance to the sensor of the OCT device. Each returning wave, thus produces a reflectivity profile in the axial dimension, also called an A-scan. By combining multiple axial A-scans, a cross-sectional tomograph of the retina also known as the B-scan can be achieved. (5) Modern spectral-domain OCT devices using a Fourier transformation, that do not require a reference arm to calculate the depth of a structure, are able to provide scans with a resolution below 5 µm. Figure 2B shows a retinal scan and the segmentation into the corresponding retinal layers. OCT measures, which evaluate retinal damage via pRNFL and combined ganglion cell-inner plexiform (GCIPL) volume, serve as a surrogate for damage of retinal axons and ganglion cells. (17,19,25,26)
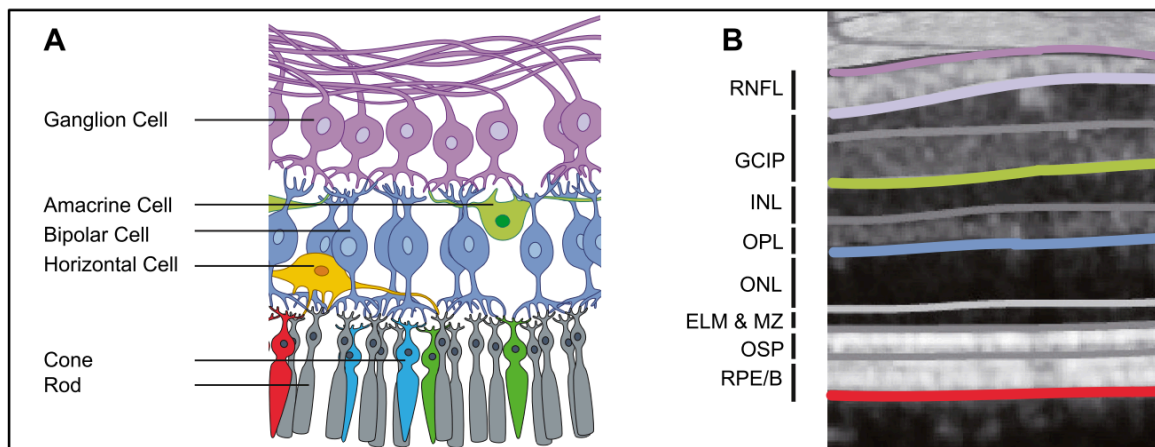

Figure 2: *Schematic view of retinal layers (A) with corresponding optic coherence tomography measurement (B).*

RNFL = retinal nerve fiber layer, GCIPL = combined ganglion cell-inner plexiform layer, INL = inner nuclear layer, OPL = outer plexiform layer, ONL = outer nuclear layer, ELM & MZ = external limiting membrane and myoid zone, OSP = outer segments of photoreceptors (ellipsoid zone), RPE/B = retinal pigment epithelium and Bruch's complex. Taken from Oertel et al 2018 (27)

Together MRI and OCT represent a promising model to evaluate optic pathway degeneration. Previous studies have shown that MRI detects changes of the optic nerve whether in the acute phase of optic neuritis or in the consecutive time after the attack. While an initial swelling at onset of optic neuritis increases the area of the optic nerve, it declines over time to manifest atrophy. (14–16,18,24) Studies combining MRI with OCT to evaluate axonal damage in optic nerve atrophy reported correlations between MRI derived measures and pRNFL, suggesting that MRI is sensitive to axonal loss as a cause of optic nerve atrophy. (19,24–26) In aquaporin 4-IgG (AQP4-IgG) seropositive NMOSD and MS, microstructural tissue alterations in the retina, optic nerves and radiations have been described. Their correlation underlines the case of trans-synaptic optic pathway degeneration spreading from the optic nerves, over the optic chiasm, to the OR in NMOSD. (6,9,28) Such microstructural tissue alterations have also been supported in patients without a history of optic neuritis. (6,9,27–30) Both, MRI and OCT measures of optic pathway atrophy have been found to be correlated with clinical measures of visual function and, thus, are used to indicate functionally relevant changes. (19,25,27)

Optic chiasm evaluation in MRI

The optic chiasm represents a promising measure of optic pathway degeneration. It is less vulnerable to motion artefacts and is consistently surrounded by cerebrospinal fluid, which reduces the problem of contrast heterogeneity. It is less variable in morphology, larger in dimension and, thus, a relatively simple target for MR based measurements. Figure 3 shows the optic chiasm surrounded by cerebrospinal fluid of the suprasellar cistern. Furthermore, the optic chiasm accumulates all axons from both sides anteriorly connected to the retina, forming the optic nerves and posteriorly passing on to the optic tracts as illustrated in Figure 1. Accordingly, effects of axonal changes due to optic neuritis and following anterograde trans-synaptic degeneration along the optic nerve accumulate in the optic chiasm. It hence represents a single structure where neurodegenerative changes following optic neuritis within the anterior optic

pathway might be well detectable. Consequently, the assessment of the optic chiasm could simplify optic nerve atrophy evaluation by reducing the region of investigation from multiple technically demanding structures to a single easily accessible structure. Nevertheless, only few studies focused on the assessment of optic chiasm dimensions. The most commonly used optic chiasm measures are optic chiasm area, width and height. (18,20,21,31) While some research groups performed optic pathway assessment to estimate neurodegeneration on the basis of T2-weighted sequences (14–16,19), others preferred T1-weighted images, especially when aiming to visualize the optic chiasm. (18,20,21,31) T2-weighted images have high signal intensities from CSF, which may lead to a blur at the edge of the optic chiasm. Consequently, the nerve sheath might mistakenly be included in the segmentation, which leads to an approximate 20% increase in optic nerve area when comparing a short tau inversion recovery sequence with a fast fluid-attenuated inversion recovery (FLAIR) sequence. (14) Although a FLAIR sequence might provide a quick work around for segmentation problems arising from high CSF intensities, a high resolution T1-weighted MRI sequence was chosen in this study. This sequence is part of the standard radiologic exam at our institution and is broadly available. It allows a sufficient optic chiasm assessment without further dedicated MRI fat-saturated acquisition sequences. Furthermore, its nearly isotropic voxel size, allows to prevent shortcomings in the multiplanar reconstruction.

Objectives

The aim of this study was to assess whether neurodegenerative changes in the anterior optic pathway can be detected by assessing optic chiasm measures. We therefore hypothesized that neurodegenerative changes of the anterior optic pathway manifest in a reduction of optic chiasm dimensions and that the evaluation of optic chiasm dimensions in conventional 3D-T1w MR images is sensitive to neurodegenerative changes in the anterior optic pathway. To test these hypotheses, we used NMOSD as a model for severe optic pathway damage and compared

different optic chiasm measures (area, width, left, central, right and total height) between AQP4-IgG seropositive NMOSD patients with and without history of optic neuritis (NMOSD-ON and NMOSD-NON) and healthy control participants. In addition, we investigated the association of optic chiasm measures with structural measures of the anterior optic pathway and clinical measures in NMOSD-ON.

Materials and Methods

The present study was approved by the local ethics committee (Ethikkommission der Charité – Universitätsmedizin Berlin; EA1/131/09) and conducted according the declaration of Helsinki and applicable German law. All participants gave written informed consent.

Study population

Data of 78 NMOSD patients acquired from an ongoing longitudinal prospective observational cohort study at the NeuroCure Clinical Research Center, Charité-Universitätsmedizin Berlin (recruited from May 2013 to January 2018) were screened for eligibility. All patients i) were 18 years or older and ii) had a diagnosis of AQP4-IgG seropositive NMOSD according to the current panel criteria (12) and iii) either had a last optic neuritis attack at least five months prior to MRI or did not have a history of optic neuritis. AQP4-IgG status was determined by a cell-based assay (Euroimmun, Lübeck, Germany). Patients with AQP4-IgG seronegative (n=25) antibody status, unknown antibody status and/or incomplete clinical data (n=10), lacking MRI data (n=3) or last optic neuritis attack within five months prior to MRI (n=1) were excluded. 39 patients exclusively with AQP4-IgG seropositive NMOSD and 37 age- and sex-matched healthy control participants were included in this study (Table 1). All healthy control participants were 18 years or older, had ophthalmologic testing and no history of neurological or ophthalmological diseases.

MRI Acquisition

MRI data were acquired on the same 3 T scanner (MAGNETOM Trio, A Tim System, Siemens) at the Berlin Center for Advanced Neuroimaging using a volumetric high-resolution T1 weighted Magnetization Prepared Rapid Gradient Echo sequence (MPRAGE) (Repetition Time = 1900 ms, Echo Time = 3.03 ms, Inversion Time = 900 ms, Field of view = 256×256 mm^2, matrix 256×256, slice thickness 1 mm), as well as a volumetric high-resolution FLAIR

sequence (Repetition Time = 6000 ms, Echo Time = 388 ms, Inversion Time = 2100 ms, Field of view = 256×256 mm², matrix 256×256, slice thickness 1 mm). Optic chiasm and optic nerve measurements were performed on reconstructed 3D MPRAGE images. Lesion load was assessed on FLAIR images of all patients, which were checked and verified for total lesion count and lesion volume by two expert raters under the supervision of a board-certified radiologist. Quantification of lesions of FLAIR images were performed using ITK-SNAP 3.2 (www.itksnap.org; accessed October 10, 2018).

Optic Chiasm Measures and Optic Nerve Diameter

Since no standardized method to assess optic chiasm dimensions in conventional MRI was available, we evaluated previous studies on optic chiasm dimensions (18,21,31) in order to define an appropriate method. In preliminary considerations and trials, we observed that the definition of measurement locations along the course of the optic pathway and angulations of the planes to it influences the results. Varying angles (not perpendicular) of the coronal plane to the course of the optic pathway at varying measure locations result in varying values of optic chiasm dimensions measured in this plane.

Consequently, a standardized protocol focused on reducing the variance of these crucial factors was used for optic chiasm dimension measurements: First the central point of the optic chiasm was determined on all 3 planes. The axes of the planes were reoriented to the course of the optic pathway, so that they were perpendicular to the orientation of the individual optic chiasm in the central point. On the individually reoriented transverse plane, optic chiasm area, heights and width were measured. Width was defined as the diameter along the adjusted frontal axis. Heights were measured perpendicularly to that diameter: central height at the middle, the lateral heights at the maximal diameter left and right to the center. Figure 3 illustrates how axes were adjusted and how optic chiasm dimensions were measured.
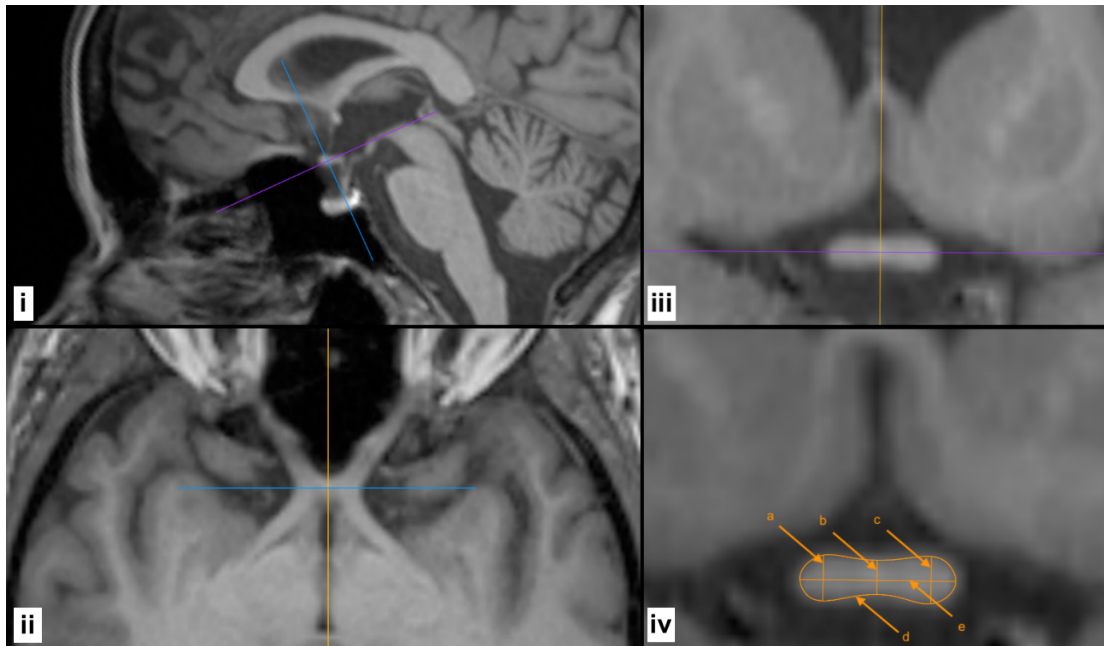
Figure 3: *Adjustment of axis for optic chiasm MRI measurements.*

Shown are optic pathways in individually reoriented i) sagittal, ii) axial, iii) coronal planes to illustrate how axis were adjusted perpendicularly to the orientation of the optic chiasm in the center point. iv) shows a sample optic chiasm measurement (a=right, b=central, c=left height, d=area, e=width). Adapted from Juenger et al., Eur Radiol 2020 (1)

Optic nerve diameters were measured in the cisternal segment 7 mm anterior to the previously defined central point of the optic chiasm perpendicular to the optic nerve course. Figure 4 illustrates how the measurement point along the optic nerve was defined and how the diameter was measured. Optic nerve measurements were conducted in the cisternal segment, since image quality issues due to contrast heterogeneity and motion artefacts in the orbital part of the optic nerve rendered its orbital evaluation difficult in 25% of the patients.

Measurements were performed using region-of-interest software from Horos version 3.3.2 (https://www.horosproject.org; accessed October 10, 2018). All measurements were performed by one rater (Valentin Jünger), blinded to clinical data, after training with Michael Scheel, a neuroradiologist with more than 8 years of experience. For the interrater reliability analysis, two raters (Valentin Jünger and Meera Chikermane) measured optic chiasm dimensions in 10

randomly selected healthy control participants and intraclass correlations (ICC) were calculated.
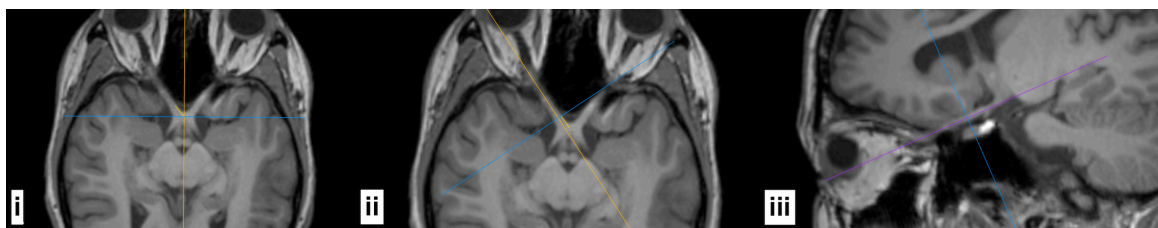

Figure 4: *Adjustment of axis for optic nerve MRI measurement.*

i, ii, iii illustrate how axis were adjusted perpendicularly to the orientation of the optic nerve. Shown are optic pathways in individually reoriented i, ii) axial and iii) sagittal planes to illustrate how axis were adjusted perpendicularly to the orientation of the optic nerve 7mm anterior of the center point of the optic chiasm. Adapted from Juenger et al., Eur Radiol 2020 (1)

Clinical Assessment

Neurological disability was graded on the Expanded Disability Status Scale (EDSS), including the visual functional system score according to the Neurostatus definitions. Raters were under the supervision of board-certified neurologists. The global neurological examination also included assessment of optic neuritis history using clinical criteria. Visual acuity was tested monocularly under phototopic conditions using retroilluminated Early Treatment in Diabetes Retinopathy Study charts at a four-meter distance. The logarithm of the minimum angle of resolution (logMAR) served as a measure of visual function. A lower logMAR value corresponds to a smaller perceived angle of resolution and thus to better visual acuity. Visual acuity data was included only from patients where best correction was used (n=30).

Optical Coherence Tomography Measures

All OCT data were acquired on a spectral domain OCT device (Spectralis, Heidelberg Engineering) with automated real-time function. No pupil dilatation was used. We report the

OCT acquisition settings and scanning protocol according to the APOSTEL recommendations (32): The pRNFL thickness was measured using 3.4-mm ring scans around the optic nerve head (12°, 1536 A-scans, $9 \leq ART \leq 100$). The GCIPL volume was measured using a 6-mm diameter cylinder around the fovea from a macular volume scan (25°x30°, 61 vertical B-scans, 768 A-scans per B-scan, ART = 15). Segmentation of the pRNFL and the intraretinal layers in the macular scan was performed semi-automatically using software provided by the optical coherence tomography manufacturer (Eye Explorer 1.9.10.0 with viewing module 6.0.9.0; Heidelberg Engineering). Quality was evaluated according to the OSCAR-IB criteria. (33) Two patients did not have OCT data. Eight eyes from six NMOSD-ON had to be excluded due to incidental findings or quality reasons. Only the macular scan from two additional NMOSD-ON eyes was excluded due to quality reasons.

Statistics

Proportional group differences were tested with χ^2 test for sex and with ANOVA test for age. For comparison of ordinal and continuous measurements, group-wise comparison were performed using Kruskal-Wallis and ANOVA tests, respectively. Group comparison of optic chiasm dimensions was corrected for multiple comparison using the Holm-Bonferroni method. The variations of the individual metrics were compared within the healthy control participants using a coefficient-of-variation (CoV) computed according to

$$\text{CoV} = \frac{standard\,deviation\,of\,the\,individual\,metric}{mean\,of\,the\,individual\,metric}$$

and served as an indicator of variation in the individual optic chiasm measures. Sensitivity to optic nerve atrophy of individual optic chiasm measures was evaluated with receiver operating characteristics (ROC) analysis, including area-under-the-curve (AUC) comparison using DeLong method. Association analysis of individual optic chiasm measures with the T2 lesion load, the SIENAX V-scaling factor (34) for head size and gender as potential influencing factors, mean optic nerve diameter, mean pRNFL thickness, mean GCIPL volume, visual

function (mean logMAR) and disease duration was performed with the Pearson correlation test, association with the number of optic neuritis attacks with the Spearman test.

Statistical analyses were performed and plots and graphs were generated by Valentin Jünger using R software, version 3.5.1. (http://www.r-project.org/; accessed October 10, 2018) with the tidyverse (https://cran.r-project.org/web/packages/tidyverse/index.html; accessed October 10, 2018), ggpubr (https://cran.r-project.org/web/packages/ggpubr/index.html; accessed October 10, 2018) and pROC packages (https://cran.r-project.org/web/packages/pROC/index.html; accessed October 10, 2018). Statistical significance was set at a p-value < 0.05.

Results

Demographics

Table 1 shows the demographic and clinical characteristics of the study cohort. No significant differences of sex distribution, age and physical disability were found between groups. 14 patients had no history of optic neuritis. Of 25 NMOSD-ON patients, 11 had a history of bilateral optic neuritis, 8 had a history of optic neuritis in the right eye, whereas 6 had a history of optic neuritis in the left eye. The median time since the last episode of optic neuritis attack was 4.9 years, the minimum was 6 months. Optic nerve diameters were smaller in NMOSD-ON compared to healthy control participants ($p<0.0001$), in NMOSD-ON compared to NMOSD-NON ($p<0.01$), but not in NMOSD-NON compared to healthy control participants ($p>0.05$).

Table 1: *Demographics and clinical characteristics.*

	HC	NMOSD-NON	NMOSD-ON	*p*
Number	37	14	25	-
Age, years (mean, SD)	47.8 (12.6)	53.8 (12.5)	48.09 (14.9)	0.33
Sex (F/M) (% female)	30/7 (81%)	14/0 (100%)	21/4 (84%)	0.22
Disease Duration, years (median, range)	-	-	7.1 (3 – 34.1)	
Number of ON (median, range)	-	-	2 (1 - 12)	-
Time since first ON, years (median, range)	-	-	6.9 (3.4 - 32.2)	-
Time since last ON, years (median, range)	-	-	4.9 (0.5 - 13.2)	-
ON Involvement, bilateral/unilateral	-	-	11/14 (8 right / 6 left)	-
Optic Nerve Diameter, mm (mean, SD)	8.37 (0.50)	8.13 (0.90)	7.06 (1.23)	<0.001
pRNFL, µm (mean, SD)	91.99 (15.10)	97.96 (10.13)	67.57 (17.92)	<0.001
GCIPL mm^3 (mean, SD)	1.83 (0.28)	1.88 (0.14)	1.49 (0.25)	<0.001
Visual acuity, logMAR (mean, SD)	-0.01 (0.21)	-0.15 (0.21)	0.30 (0.63)	0.04
Visual Functional System Score (median, range)	-	0 (0 -2)	1 (0 - 6)	<0.001
EDSS (median, range)	-	3 (1 – 7)	4 (0 - 6.5)	0.71

p-values are group-wise comparisons. HC = healthy controls; NMOSD-ON = neuromyelitis optica patients with history of optic neuritis; NMOSD-NON = neuromyelitis optica patients without history of optic neuritis; ON = optic neuritis; pRNFL = peripapillary retinal nerve fiber layer; GCIPL = combined ganglion cell-inner plexiform layer; logMAR = logarithm of the minimum angle of resolution; EDSS = Expanded Disability Status Scale. Adapted from Juenger et al., Eur Radiol 2020 (1)

Group Comparison and Receiver Operating Characteristics

NMOSD patients presented smaller optic chiasm dimensions than healthy control participants. Figure 5 shows the optic chiasm of NMOSD-ON, NMOSD-NON and healthy control participants to illustrate the reduction of optic chiasm dimensions in NMOSD.
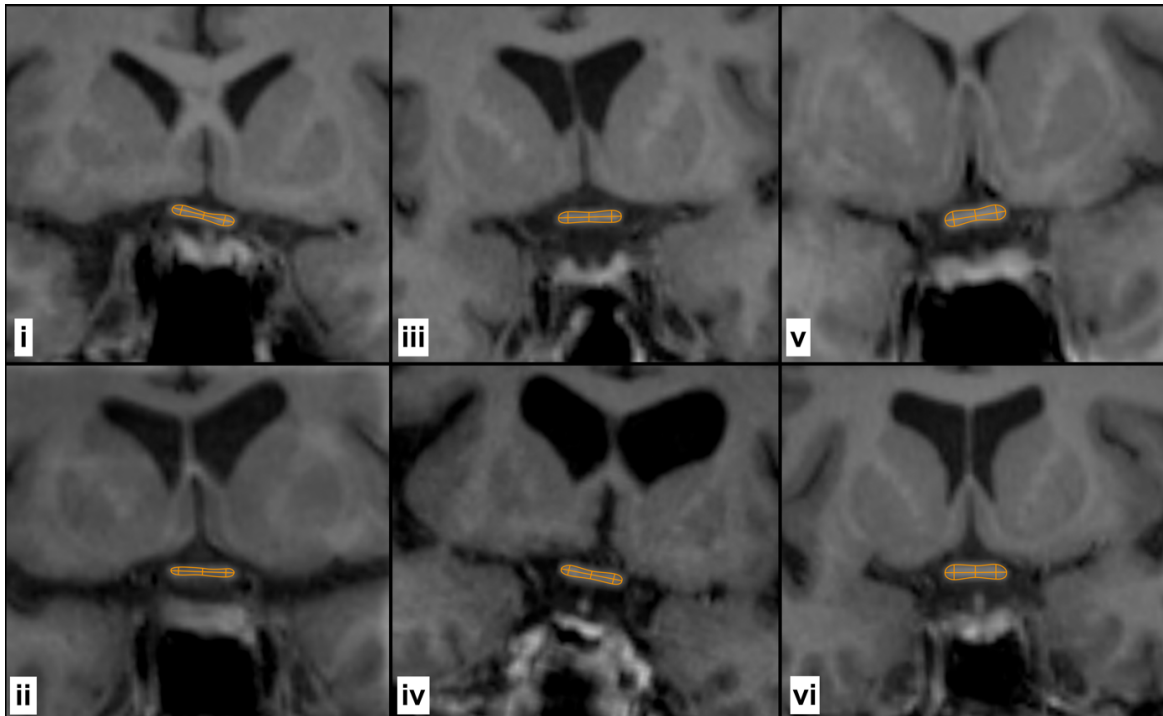

Figure 5: *Sample MRI measurements of optic chiasm dimensions*

Shown are optic chiasms in individually reoriented transversal planes of NMOSD-ON (i, ii), NMOSD-NON (iii, iv) and healthy control subjects (v, vi). Sample measurements of optic chiasm dimensions are shown using a freeform region-of-interest software from Horos. Adapted from Juenger et al., Eur Radiol 2020 (1)

Specifically, all optic chiasm measures except width were significantly smaller in all group comparisons (NMOSD-ON vs. HC: $p<0.0001$, NMOSD-NON vs. HC: $p<0.01$ and NMO-ON vs. NMO-NON: $p<0.03$), as shown in Table 2 and Figure 6. When correcting for multiple comparisons (corrected $p=0.003$), this remained significant for all measures for healthy control

participants vs. NMOSD-ON, for all measures except left height for healthy control participants vs. NMOSD-NON and for area for NMOSD-NON vs. NMOSD-ON.

Table 2: Optic chiasm measures.

	HC	NMOSD-NON	NMOSD-ON	HC vs. NMOSD-NON	HC vs. NMOSD-ON	NMOSD-NON vs. NMOSD-ON	CoV	ICC
Left Height (CI, mm)	2.77 (0.35)	2.34 (0.53)	1.94 (0.48)	t=2.77 p=0.01	t=7.49 p<0.0001	t=2.36 p=0.03	0.12	0.71
Central Height (CI, mm)	1.93 (0.32)	1.55 (0.39)	1.22 (0.32)	t=3.27 p<0.001	t=8.63 p<0.0001	t=2.70 p=0.013	0.16	0.51
Right Height (CI, mm)	2.65 (0.36)	2.20 (0.46)	1.79 (0.43)	t=3.31 p=0.003	t=8.23 p<0.0001	t=2.79 p=0.008	0.14	0.77
Width (CI, mm)	12.23 (1.15)	12.17 (1.05)	11.43 (1.87)	t=0.17 p=0.56	t=1.91 p=0.059	t=1.59 p=0.18	0.09	0.95
Area (CI, mm^2)	27.07 (3.50)	22.26 (4.65)	16.89 (4.44)	t=3.51 p=0.003	t=9.61 p<0.0001	t=3.51 p=0.001	0.13	0.89
Total Height (CI, mm)	7.35 (0.90)	6.09 (1.33)	4.94 (1.14)	t=3.27 p=0.003	t=8.86 p<0.0001	t=2.73 p=0.009	0.12	0.76

Shown are means of optic chiasm measures. p- and t-values are derived from t-tests. Corrected p=0.003. CI = 95% Confidence Interval; HC = healthy controls; NMOSD-ON = neuromyelitis optica patients with history of optic neuritis; NMOSD-NON = neuromyelitis optica patients without history of optic neuritis; CoV = coefficient-of-variation; ICC = intraclass correlations. Adapted from Juenger et al., Eur Radiol 2020 (1)
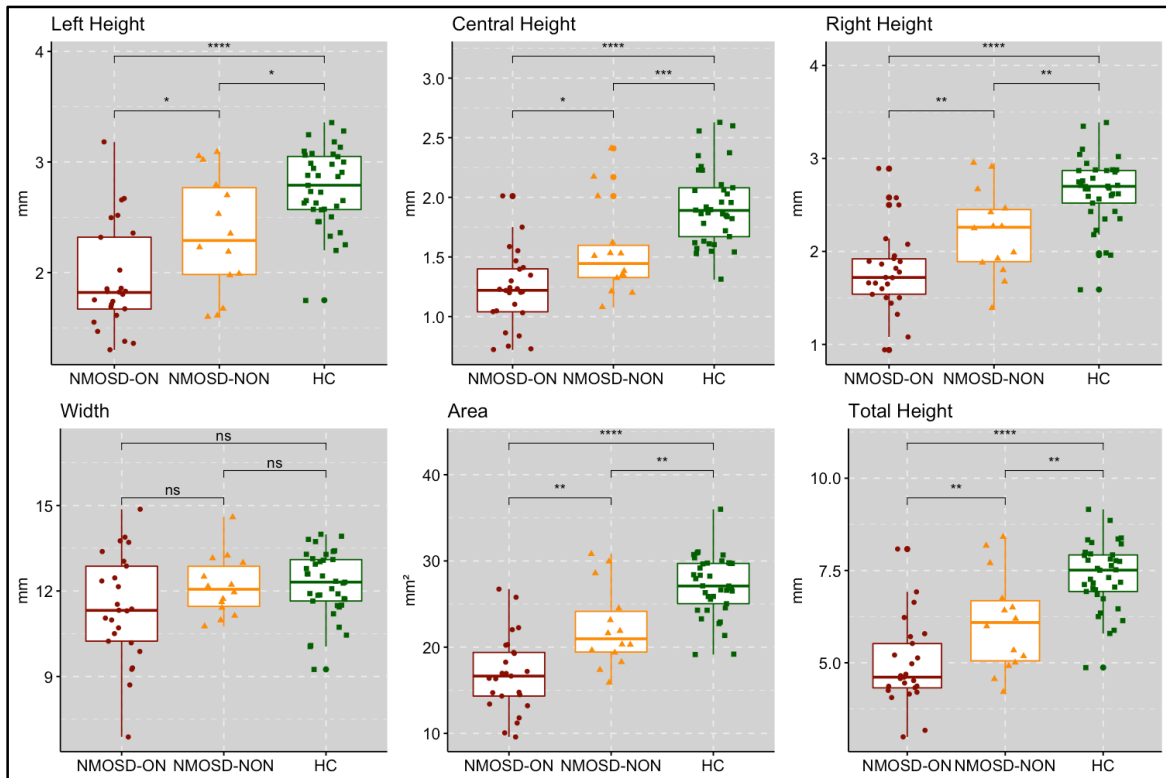
Figure 6: Comparison of optic chiasm measures.

Shown are boxplots to illustrate group differences in optic chiasm heights width and area between neuromyelitis optica spectrum disorders patients with optic neuritis (NMOSD-ON, red), without optic neuritis (NMOSD-NON, orange) and healthy control subjects (HC, green). ns: p>0.05, * p≤0.05, ** p≤0.01, *** p≤0.001, ****p≤0.0001. Adapted from Juenger et al., Eur Radiol 2020 (1)

Optic chiasm measures were not associated with the T2 lesion load (r=-0.35, p>0.09), the number of optic neuritis attacks (r=-0.31, p>0.13), the number of optic neuritis attacks per side (r=-0.09, p>0.13), head size (r<0.08) or gender (p>0.23). Thus, no correction for lesion load, head size or sex was performed.

A ROC analysis was conducted to test the ability of the optic chiasm to predict the presence of damage in the anterior optic pathway, namely to differentiate between groups. Figure 7 show

the ROC curves, illustrating this ability on the basis of each individual optic chiasm measure. Optic chiasm area and optic chiasm heights have comparable AUC values for each group (NMOSD-ON vs. HC: AUC>0.92; NMOSD-NON vs. HC: AUC>0.74; NMO-ON vs. NMO-NON: AUC>0.71), whereas width has lower AUC values, as shown in Table 3 and Figure 7. AUC comparison using DeLong method and variation comparison using the CoV of the best performing measures, revealed no significant difference. An optic chiasm area smaller than $22.5mm^2$ yielded a sensitivity of 0.92 and a specificity of 0.92 in separating chiasms of NMOSD-ON from healthy control participants.

Table 3: *Receiver Operating Characteristics Analysis.*

HC vs. NMOSD-ON	Area	Width	Left Height	Central Height	Right Height	Total Height
AUC	0.95	0.64	0.90	0.95	0.92	0.94
95% CI	0.91 - 1.00	0.49 - 0.79	0.81 - 0.98	0.89 - 1.00	0.85 - 1.00	0.87 - 1.00
p-value AUC comparison	-	<0.01	0.02	0.78	0.16	0.40
HC vs. NMOSD-NON	**Area**	**Width**	**Left Height**	**Central Height**	**Right Height**	**Total Height**
AUC	0.78	0.55	0.74	0.80	0.78	0.77
95% CI	0.57 - 0.92	0.38 - 0.73	0.52 - 0.88	0.59 - 0.95	0.62 - 0.94	0.60 - 0.94
p-value AUC comparison	-	0.08	0.31	0.49	0.93	0.77
NMOSD-ON vs. NMOSD-NON	**Area**	**Width**	**Left Height**	**Central Height**	**Right Height**	**Total Height**
AUC	0.81	0.63	0.71	0.74	0.76	0.76
95% CI	0.69 - 0.95	0.46 - 0.80	0.54 - 0.89	0.59 - 0.90	0.57 - 0.90	0.60 - 0.92
p-value AUC comparison	-	0.08	0.06	0.19	0.29	0.14

Shown are area under the curve (AUC), 95% confidence interval (CI) and p-value for AUC comparison using DeLong method with optic chiasm area as reference. HC = healthy control subjects; NMOSD-ON = neuromyelitis optica patients with history of optic neuritis; NMOSD-NON = neuromyelitis optica patients without history of optic neuritis. Adapted from Juenger et al., Eur Radiol 2020 (1)
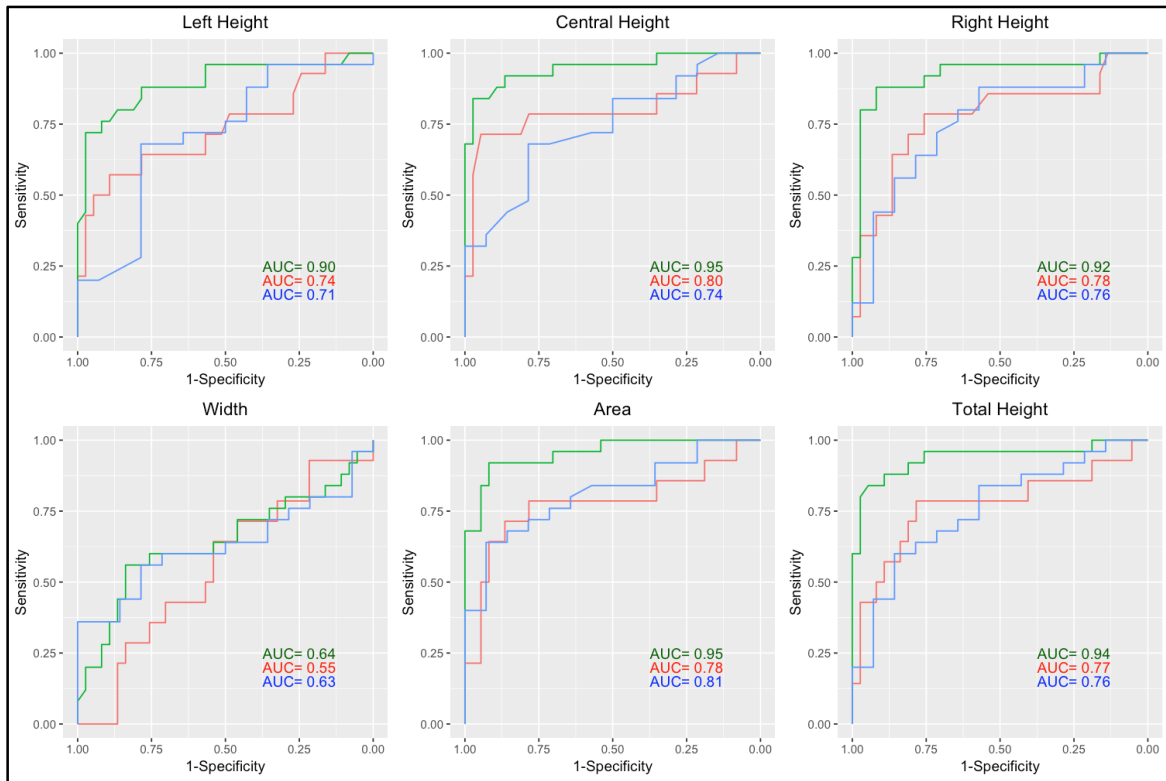
Figure 7: *Receiver operating characteristics analysis of optic chiasm measures.*

ROC curves show the ability of the optic chiasm to predict the presence of damage in the anterior optic pathway, namely to differentiate between groups, on the basis of each individual optic chiasm measure. Each line represents one group differentiation: green lines HC vs. NMOSD-ON, red lines HC vs. NMOSD-NON, blue lines NMOSD-ON vs. NMOSD-NON; ON = optic neuritis. HC = healthy controls; NMOSD-ON = neuromyelitis optica patients with history of optic neuritis; NMOSD-NON = neuromyelitis optica patients without history of optic neuritis; ROC = Receiver operating characteristics. Adapted from Juenger et al., Eur Radiol 2020 (1)

Associations with structural measures and clinical parameters

Table 4 summarizes the association analysis within the NMOSD-ON group. Higher optic chiasm measures were associated with bigger optic nerve diameter, better visual acuity and better OCT measures. This was most prominent for optic chiasm area: Higher values significantly correlated with bigger optic nerve diameter (r=0.4, p=0.047), better logMAR (r=-0.57, p=0.013), thicker pRNFL (r=0.59, p=0.003), bigger GCIPL (r=0.55, p=0.007) and shorter disease duration (r=-0.5, p=0.012). Within optic chiasm heights, only central height was significantly associated with GCIPL (r=0.46, p=0.028). Figure 8 illustrates the relationship between optic chiasm area and pRNFL thickness, as well as logMAR.

Table 4: *Associations of optic chiasm measures and visual acuity, optic nerve diameter and optical coherence tomography measures for NMOSD-ON patients.*

	Area	**Width**	**Left Height**	**Central Height**	**Right Height**	**Total Height**
Visual acuity (logMAR)	r=-0.57 p=0.013	r=-0.53 p=0.023	r=-0.05 p=0.84	r=-0.43 p=0.079	r=-0.21 p=0.41	r=-0.22 p=0.39
Optic nerve diameter	r=0.4 p=0.047	r=0.75 p<0.001	r=-0.06 p=0.78	r=-0.09 p=0.68	r=0.09 p=0.66	r=-0.03 p=0.87
pRNFL thickness	r=0.59 p=0.003	r=0.54 p=0.008	r=0.15 p=0.49	r=0.38 p=0.07	r=0.30 p=0.16	r=0.28 p=0.19
GCIPL volume	r=0.55 p=0.007	r=0.33 p=0.13	r=0.19 p=0.39	r=0.46 p=0.028	r=0.34 p=0.11	r=0.33 p=0.12

r values are Pearson's correlation coefficients. NMOSD-ON = neuromyelitis optica patients with history of optic neuritis; logMAR = logarithm of the minimum angle of resolution; pRNFL = peripapillary retinal nerve fiber layer; GCIPL = combined ganglion cell-inner plexiform layer. Adapted from Juenger et al., Eur Radiol 2020 (1)
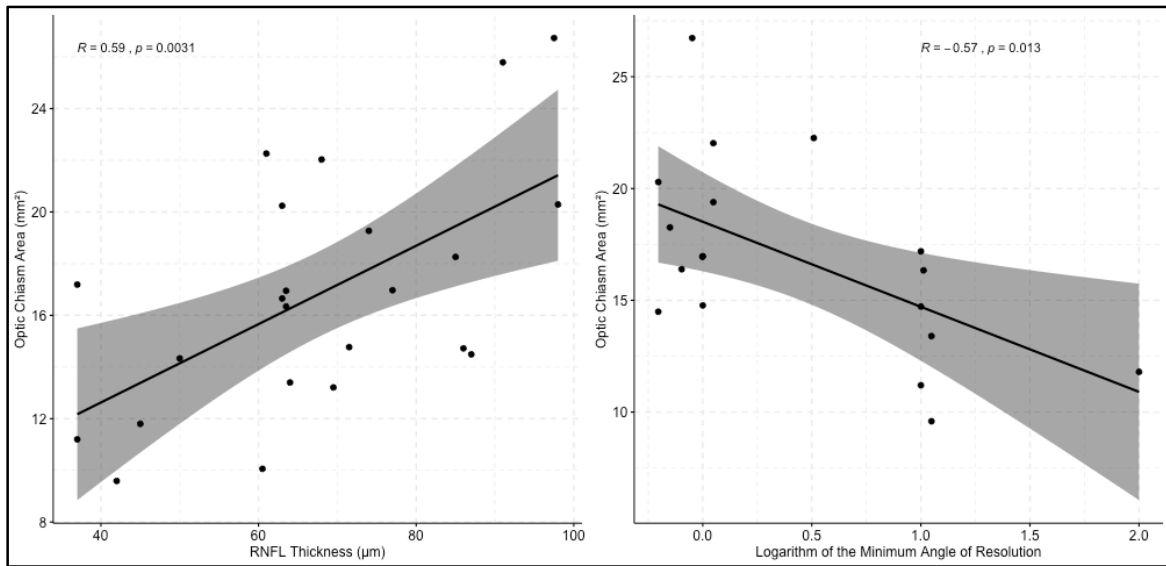
Figure 8: *Relationship between MRI measured optic chiasm area and pRNFL thickness and logMAR.*

The scatterplot demonstrates a positive correlation between MRI measured optic chiasm area and OCT measured pRNFL thickness and a negative correlation to the logMAR in patients with optic nerve atrophy. Included are regression lines and 95% confidence interval; logMAR = logarithm of the minimum angle of resolution; pRNFL = peripapillary retinal nerve fiber layer; R = correlation coefficient

Discussion

We evaluated optic chiasm dimensions as imaging marker of anterior optic pathway damage. We demonstrated significant group differences between NMOSD patients and healthy control participants and strong associations of optic chiasm measures with structural measures of the anterior optic pathway and clinical parameters. Our data show that optic chiasm assessment in conventional 3D-T1w MR images is sensitive to anterior optic pathway damage. Hence, optic chiasm dimensions are easily accessible and sensitive markers of anterior optic pathway damage.

Optic chiasm dimensions and group differences

Optic chiasm dimension values for healthy control participants presented in our study are similar to recently published data. (31) A previous study by Wagner et al. (21), however, reported slightly higher optic chiasm width and area values. This study excluded optic chiasm height due to a high degree of variance. Notably, unlike our study, Wagner et al. did not account for the transverse course of the optic pathway and did not define precise measurement locations. Thus, the coronal plane would be at varying angles (not perpendicular) to the course of the optic pathway at which optic chiasm assessment results in higher values and variance. Furthermore, our study employed a higher resolution MRI sequence, which may have an impact on values and variance, since limited spatial resolution can induce partial volume effects. (35) This effect is due to the limited resolution of the imaging system and especially apparent when imaging small objects. Given a selected MRI sequence, the signal obtained from a specific voxel is determined by the entire contents of the anatomical volume it represents. As long as the anatomical volume represented by the voxel contains only a single tissue type, the signal of that voxel will be characteristic of the represented tissue type. On the other hand, if the anatomical volume contains more than a single tissue type, such as at the edge of the structure, partial volume effects may occur. The signal of that voxel will then be composed of the different tissue

types contained in the represented anatomical volume. In the case of optic chiasm segmentation, partial volume effects might occur at the edges of the structure, where the anatomical volume represented by the voxel contains nervous tissue and cerebrospinal fluid. It is, thus, plausible, that the image resolution affects the variance of optic chiasm measurements.

Optic chiasm heights and area showed differences between all groups. This is in line with earlier investigations suggesting that optic nerve dimensions discriminate optic neuritis patients from controls. (14,17) Optic chiasm assessment, as suggested in our study, only requires a standard and broadly available MRI sequence (3D T1-weighted MPRAGE) and measures a rather fixed structure less vulnerable to motion artefacts compared to the previously used orbital optic nerves. (14,15,17,19) Note that in this study, optic nerve diameters were measured in the cisternal segment 7mm anterior to the optic chiasm, since contrast heterogeneity and motion artefacts in the orbital part rendered orbital assessment difficult in 25% of the patients. The observation that smaller optic chiasm dimensions were also found in NMOSD-NON (compared to healthy control participants and NMOSD-ON) supports microstructural changes in the optic pathway independent of optic neuritis (27), which have been described in NMOSD. (6,28–30)

In concordance with a study by Harrigan et al. (17), the optic nerve diameter was smaller in patients with history of optic neuritis compared to healthy control participants but not in patients without optic neuritis. Although this should not be overstated in consideration of the small NMOSD-NON sample size, this might indicate that microstructural changes independent of optic neuritis, including anterograde degeneration originating from anterior optic pathway damage but also retrograde degeneration originating from posterior optic pathway damage, might accumulate in the optic chiasm.

Receiver operating characteristics analysis

An ROC curve was calculated to test the ability of the optic chiasm to predict the presence of damage of the anterior optic pathway, namely its ability to distinguish optic chiasm dimensions from patients and those from healthy control subjects. The AUC values obtained from the ROC analyses for optic chiasm area and heights (> 0.92 for NMOSD-ON vs. HC and > 0.80 for NMOSD-NON vs. HC) discriminate well between affected and unaffected optic pathways. This indicates that optic chiasm measures are sensitive to anterior optic pathway damage. The observation that no association between optic neuritis attacks per side and optic chiasm heights was found, highlights the fact that optic chiasm assessment accumulates pathophysiological processes of both sides and does not provide information on the origin of the fibers. The presented optic chiasm area cut-off value of 22.5 mm^2 separated affected optic chiasms from unaffected ones with a sensitivity of 0.92 and a specificity of 0.92. It should be emphasized that this value needs to be understood as a study-specific value, and further work in a larger cohort would be required to determine a value suitable for current clinical practice or making clinical diagnosis. The extent of degenerative optic pathway changes specific to each cohort and each inflammatory autoimmune central nervous disease seems to bias the cut-off value, which therefore needs to be evaluated further in studies with lager cohorts. Alongside MRI evaluation of the entire central nervous system, the inclusion of parameters obtained from clinical examination, ophthalmologic visits and immunological analysis are crucial for a final interpretation or diagnosis of focal optic neuritis or NMOSD.

Association with structural measures clinical parameters

We observed associations between optic chiasm dimensions with structural measures of the anterior optic pathway and clinical parameters. Specifically, the observed correlation between higher optic chiasm area and better visual acuity (r=-0.57), thicker pRNFL (r=0.53) and bigger GCIPL (r=0.55) in NMOSD are similar to the associations previously reported on optic nerve

dimensions (r=-0.50, r=0.66, r=0.59) in multiple sclerosis. (19) Alongside findings suggesting that axonal loss is a major substrate of MRI-detected optic pathway atrophy after optic neuritis (18,19,25,26), the association between structural measures of the anterior optic pathway such as pRNFL (a measure for retinal axons) and optic chiasm dimensions implies that the assessment of the optic chiasm is sensitive to atrophic changes of the anterior optic pathway. However, axonal loss is not the only substrate of neurogenerative processes. Gliosis and changes in water content also contribute to MRI-detected changes after optic neuritis. (36) The associations of optic chiasm area with clinical measures such as visual function and disease duration suggest a role for the optic chiasm as an imaging marker of neurodegenerative damage in the optic pathway with potential functional relevance.

Possible clinical applications and new scientific questions

Optic chiasm measures, as demonstrated in our study, are easy to obtain through a single and simple measurement. This is beneficial, since the presented method does not require additional and time consuming sequences, nor complex imaging post-processing procedures. While it does not provide information on the origin of the fibers and evaluation of focal optic nerve damage might better be achieved by direct measurement at the sight of inflammation, it accumulates neurodegeneration from both sides of the anterior optic pathway causing observable impairment. Thus, it extends the amount of information from a single measurement in the conventional and clinical standard scan. Broad accessibility and uncomplicated implementation of the present method is, furthermore, promising for cooperation between research centers. Optic chiasm measures might be useful markers to facilitate such approaches, as they can be assessed in a conventional MRI sequence (3D T1-weighted), that is usually part of a standard radiologic exam. Multicenter studies are viable study designs especially in diseases with a low prevalence, since they provide the opportunity to include larger cohorts of NMOSD patients and, thus, conduct more refined investigations. In addition, they allow to cancel out possible

effects resulting from differing therapeutic regimes or disease severity at different sites. Analyzing larger cohorts at multiple centers could result in a more elaborate optic chiasm area cut-off value for an application in clinical practice.

Our data provide a strong rationale for future studies on optic pathway degeneration to include the optic chiasm as an easily accessible imaging marker. This method should be validated and extended to patients with neuroinflammatory diseases other than NMOSD, such as multiple sclerosis and myelin oligodendrocyte glycoprotein antibody associated disease. In these inflammatory autoimmune central nervous system diseases, as well as in NMOSD, it could be used for monitoring of disease progression or determining therapeutic effectiveness, which is especially interesting in the era of upcoming evidence-based treatment options for NMOSD. In longitudinal studies focusing on clinical outcomes under immunomodulatory therapy, the application of the method in this matter could be addressed.

Technical refinement might further facilitate and improve the method. Advancing it to achieve a volumetry of the optic chiasm, analogously to the method presented by Avery et al. (20) seems interesting. Capturing the optic chiasm three-dimensionally would allow to assess the volume of the optic chiasm as markers of optic pathway degeneration and its sensitivity. Maintaining simple, standardized criteria to define the anterior boarders to the optic nerves and the posterior boarders to the optic tracts seems crucial to preserve the low variability in a volumetric approach. Notably, a previous work by Harrigan et al. (17) achieved a volumetric measurement of the optic nerves, but fell back to compare the nerves between MS patients and controls on the basis of the radius, a one dimensional measure, rather than its volume. It is also of note, that Harrigan et al. (17) presented an automatized method to segment the optic nerves, which is not applicable to standard of care imaging protocols and requires complex image post-processing. Through such technical automatization of the segmentation process rater depended variability inherent in manually performed measurements can be avoided. However, the image acquisition requirements, the image processing and the implementation of such a tool should be kept simple

in order not to lose the character of a broadly accessible method and its usefulness for studies across centers.

Finally, assessing degeneration in the optic chiasm and its context to changes in other sites of inflammation in NMOSD, could reveal further insights into the relationship between neurodegenerative processes in different anatomical structures and its diffusion throughout the central nervous system. Combining optic chiasm measurements with the evaluation of the spinal cord for example through the mean upper cervical cord area (37) might help to understand the interaction of neurodegeneration in these major sites of inflammation in NMOSD. It seems especially interesting to compare findings on the distribution and interaction of neurodegenerative processes between AQP4-IgG-positive NMOSD, seronegative NMOSD and other neuroinflammatory diseases to help understand possible differences of the underlying pathophysiology.

Advanced quantitative imaging methods, assessing the microstructural integrity of tissue can detect neurodegenerative changes in neuroinflammatory diseases and seem particularly promising when applied to the frequently affected visual pathway. (9,38) Diffusion tensor imaging, has been shown to detect microstructural and non-overt tissue damage in the afferent optic pathway of patients suffering from NMOSD. (9,28,38) It is based on the three-dimensional diffusion of water molecules and calculates a tensor describing their diffusion behavior. This is influenced by the directedness of the nerve fibers in the region of interest. Due to the high amount of crossing nerve fibers in the optic chiasm, impacting the overall directedness of the nerve fibers the application of diffusion tensor imaging to the optic chiasm might be technically challenging. Nevertheless, it might provide an opportunity to quantify the effect of accumulating neurodegenerative changes at the only unpaired structure of the optic pathway. This way the optic chiasm could be assessed as a structure, where inflammatory processes might be detected in early stages of disease.

Limitations

Despite the low total number of subjects included in the study owing to the low prevalence of the disease (39), a significant difference in optic chiasm measures was shown within a relatively large homogeneous cohort exclusively consisting of AQP4-IgG-positive NMOSD patients. Separate gender analysis could not be conducted due to the high proportion of female patients. This is in line with the strong female preponderance in NMOSD. (40) Optic chiasm width was measured along straight lines, which may not account for curved width morphologies. In future investigations, curved lines could be drawn, however, only few participants showed recognizable deviation from straight lines and, thus, we do not expect that this would drastically change the presented results. It should be noted, that only MRI sessions at least 6 months after last optic neuritis attack were included. Acute episodes of optic pathway inflammation might result in an increase in optic chiasm dimensions, where the application of this method does not seem adequate. The presented optic chiasm area cut-off value of 22.5 mm^2 needs to be understood as a study-specific value. For an application in current clinical practice, further work in larger cohorts including multiple centers would be required to determine a suitable, more elaborate value.

Conclusion

Our study represents an initial evaluation and assessment of optic pathway degeneration via optic chiasm measures on routine MRI scans in patients with NMOSD compared to healthy controls. It was demonstrated that the optic chiasm area seems a suitable, sensitive and reliable measure, since it is associated with structural measures of the anterior optic pathway and clinical parameters. This simple method extends the amount of information that can be obtained from conventional and clinically available scans. Our results suggest that optic chiasm dimensions are promising and easily accessible imaging markers for the assessment of neurodegenerative changes of the anterior optic pathway.

References

1. Juenger V, Cooper G, Chien C, Chikermane M, Oertel FC, Zimmermann H, Ruprecht K, Jarius S, Siebert N, Kuchling J, Papadopoulou A, Asseyer S, Bellmann-Strobl J, Paul F, Brandt AU, Scheel M. Optic chiasm measurements may be useful markers of anterior optic pathway degeneration in neuromyelitis optica spectrum disorders. Eur Radiol. 2020 Apr 26;1–11.

2. Walsh FB, Hoyt WF, Miller NR. Walsh and Hoyt's Clinical Neuro-ophthalmology. 1 / Neil R. Miller. 4th ed. Baltimore: Williams & Wilkins; 1988.

3. Zimmermann HG, Brandt AU, Paul F. Optische Kohärenztomografie in der Neurologie - Methodik und Anwendung in Forschung und Klinik [Internet]. Vol. 48, Klinische Neurophysiologie. Georg Thieme Verlag; 2017 [2020 Aug 12]. p. 211–25.

4. Jarius S, Wildemann B, Paul F. Neuromyelitis optica: Clinical features, immunopathogenesis and treatment. Clin Exp Immunol. 2014 May;176(2):149–64.

5. Schmidt F, Zimmermann H, Mikolajczak J, Oertel FC, Pache F, Weinhold M, Schinzel J, Bellmann-Strobl J, Ruprecht K, Paul F, Brandt AU. Severe structural and functional visual system damage leads to profound loss of vision-related quality of life in patients with neuromyelitis optica spectrum disorders. Mult Scler Relat Disord. 2017 Jan;11:45–50.

6. Tian D-C, Su L, Fan M, Yang J, Zhang R, Wen P, Han Y, Yu C, Zhang C, Ren H, Shi K, Zhu Z, Dong Y, Liu Y, Shi F-D. Bidirectional degeneration in the visual pathway in neuromyelitis optica spectrum disorder (NMOSD). Mult Scler J. 2018 Oct 21;24(12):1585–93.

7. Tur C, Goodkin O, Altmann DR, Jenkins TM, Miszkiel K, Mirigliani A, Fini C, Gandini Wheeler-Kingshott CAM, Thompson AJ, Ciccarelli O, Toosy AT. Longitudinal evidence for anterograde trans-synaptic degeneration after optic neuritis. Brain. 2016 Mar;139(Pt 3):816–28.

8. Gabilondo I, Martínez-Lapiscina EH, Martínez-Heras E, Fraga-Pumar E, Llufriu S, Ortiz S, Bullich S, Sepulveda M, Falcon C, Berenguer J, Saiz A, Sanchez-Dalmau B, Villoslada P. Trans-synaptic axonal degeneration in the visual pathway in multiple sclerosis. Ann Neurol. 2014 Jan;75(1):98–107.

9. Kuchling J, Brandt AU, Paul F, Scheel M. Diffusion tensor imaging for multilevel assessment of the visual pathway: possibilities for personalized outcome prediction in autoimmune disorders of the central nervous system. EPMA J. 2017 Sep;8(3):279–94.

10. Sinnecker T, Oberwahrenbrock T, Metz I, Zimmermann H, Pfueller CF, Harms L, Ruprecht K, Ramien C, Hahn K, Brück W, Niendorf T, Paul F, Brandt AU, Dörr J, Wuerfel J. Optic radiation damage in multiple sclerosis is associated with visual dysfunction and retinal thinning – an ultrahigh-field MR pilot study. Eur Radiol. 2015 Jan 17;25(1):122–31.

11. Stiebel-Kalish H, Hellmann MA, Mimouni M, Paul F, Bialer O, Bach M, Lotan I. Does time equal vision in the acute treatment of a cohort of AQP4 and MOG optic neuritis? Neurol - Neuroimmunol Neuroinflammation. 2019 Jul 21;6(4):e572.

12. Wingerchuk DM, Banwell B, Bennett JL, Cabre P, Carroll W, Chitnis T, De Seze J, Fujihara K, Greenberg B, Jacob A, Jarius S, Lana-Peixoto M, Levy M, Simon JH, Tenembaum S, Traboulsee AL, Waters P, Wellik KE et al. International consensus diagnostic criteria for neuromyelitis optica spectrum disorders. Vol. 85, Neurology.

Lippincott Williams and Wilkins; 2015. p. 177–89.

13.   Schild H. MRI made easy : (... well almost). Schering AG; 1990. 105 p.

14.   Hickman SJ, Brex PA, Brierley CMH, Silver NC, Barker GJ, Scolding NJ, Compston DAS, Moseley IF, Plant GT, Miller DH. Detection of optic nerve atrophy following a single episode of unilateral optic neuritis by MRI using a fat-saturated short-echo fast FLAIR sequence. Neuroradiology. 2001;43(2):123–8.

15.   Hickman SJ, Toosy AT, Jones SJ, Altmann DR, Miszkiel KA, MacManus DG, Barker GJ, Plant GT, Thompson AJ, Miller DH. A serial MRI study following optic nerve mean area in acute optic neuritis. Brain. 2004 Aug 19;127(11):2498–505.

16.   Hickman SJ, Brierley CMH, Brex PA, MacManus DG, Scolding NJ, Compston DAS, Miller DH. Continuing optic nerve atrophy following optic neuritis: a serial MRI study. Mult Scler. 2002 Aug 1;8(4):339–42.

17.   Harrigan RL, Smith AK, Lyttle B, Box B, Landman BA, Bagnato F, Pawate S, Smith SA. Quantitative characterization of optic nerve atrophy in patients with multiple sclerosis. Mult Scler J – Exp Transl Clin. 2017;3(3):205521731773009.

18.   Parravano JG, Toledo A, Kucharczyk W. Dimensions of the optic nerves, chiasm, and tracts: Mr quantitative comparison between patients with optic atrophy and normals. J Comput Assist Tomogr. 1993;17(5):688–90.

19.   Trip SA, Schlottmann PG, Jones SJ, Li WY, Garway-Heath DF, Thompson AJ, Plant GT, Miller DH. Optic nerve atrophy and retinal nerve fibre layer thinning following optic neuritis: Evidence that axonal loss is a substrate of MRI-detected atrophy. Neuroimage. 2006;31(1):286–93.

20.   Avery RA, Mansoor A, Idrees R, Biggs E, Alsharid MA, Packer RJ, Linguraru MG. Quantitative MRI criteria for optic pathway enlargement in neurofibromatosis type 1. Neurology. 2016;86(24):2264–70.

21.   Wagner A, Murtagh F, Hazlett K, Paley MN, Hadjivassiliou M, Wilkinson JM. Measurement of the normal optic chiasm on coronal MR images [published erratum appears in AJNR Am J Neuroradiol 1997 Aug. Am J Neuroradiol. 2014;18(4):723–6.

22.   Papadopoulou A, Oertel FC, Gaetano L, Kuchling J, Zimmermann H, Chien C, Siebert N, Asseyer S, Bellmann-Strobl J, Ruprecht K, Chakravarty MM, Scheel M, Magon S, Wuerfel J, Paul F, Brandt AU. Attack-related damage of thalamic nuclei in neuromyelitis optica spectrum disorders. J Neurol Neurosurg Psychiatry. 2019 Oct 1;90(10):1156–64.

23.   Naismith RT, Xu J, Tutlam NT, Snyder A, Benzinger T, Shimony J, Shepherd J, Trinkaus K, Cross AH, Song S-K. Disability in optic neuritis correlates with diffusion tensor-derived directional diffusivities. Neurology. 2009 Feb 17;72(7):589–94.

24.   Zhao B, Torun N, Elsayed M, Cheng AD, Brook A, Chang YM, Bhadelia RA. Diagnostic utility of optic nerve measurements with MRI in patients with optic nerve atrophy. Am J Neuroradiol. 2019 Feb 14;40(3):558–61.

25.   Manogaran P, Vavasour IM, Lange AP, Zhao Y, McMullen K, Rauscher A, Carruthers R, Li DKB, Traboulsee AL, Kolind SH. Quantifying visual pathway axonal and myelin loss in multiple sclerosis and neuromyelitis optica. NeuroImage Clin. 2016;11:743–50.

26.   Manogaran P, Hanson JVM, Olbert ED, Egger C, Wicki C, Gerth-Kahlert C, Landau K, Schippling S. Optical Coherence Tomography and Magnetic Resonance Imaging in Multiple Sclerosis and Neuromyelitis Optica Spectrum Disorder. Int J Mol Sci. 2016

Nov 15;17(11).

27.   Oertel FC, Zimmermann H, Paul F, Brandt AU. Optical coherence tomography in neuromyelitis optica spectrum disorders: potential advantages for individualized monitoring of progression and therapy. EPMA J. 2018 Mar;9(1):21–33.

28.   Oertel FC, Kuchling J, Zimmermann H, Chien C, Schmidt F, Knier B, Bellmann-Strobl J, Korn T, Scheel M, Klistorner A, Ruprecht K, Paul F, Brandt AU. Microstructural visual system changes in AQP4-antibody-seropositive NMOSD. Neurol Neuroimmunol neuroinflammation. 2017 May;4(3):e334.

29.   Akaishi T, Kaneko K, Himori N, Takeshita T, Takahashi T, Nakazawa T, Aoki M, Nakashima I. Subclinical retinal atrophy in the unaffected fellow eyes of multiple sclerosis and neuromyelitis optica. J Neuroimmunol. 2017 Dec 15;313:10–5.

30.   Oertel FC, Havla J, Roca-Fernández A, Lizak N, Zimmermann H, Motamedi S, Borisow N, White OB, Bellmann-Strobl J, Albrecht P, Ruprecht K, Jarius S, Palace J, Leite MI, Kuempfel T, Paul F, Brandt AU. Retinal ganglion cell loss in neuromyelitis optica: a longitudinal study. J Neurol Neurosurg Psychiatry. 2018 Dec 1;89(12):1259–65.

31.   Käsmann-Kellner B, Schäfer T, Krick CM, Ruprecht KW, Reith W, Schmitz BL. Anatomical differences in optic nerve, chiasma and tractus opticus in human albinism as demonstrated by standardised clinical and MRI evaluation. Klin Monbl Augenheilkd. 2003 May 1;220(5):334–44.

32.   Cruz-Herranz A, Balk LJ, Oberwahrenbrock T, Saidha S, Martinez-Lapiscina EH, Lagreze WA, Schuman JS, Villoslada P, Calabresi P, Balcer L, Petzold A, Green AJ, Paul F, Brandt AU, Albrecht P. The APOSTEL recommendations for reporting quantitative optical coherence tomography studies. Vol. 86, Neurology. Lippincott Williams and Wilkins; 2016. p. 2303–9.

33.   Schippling S, Balk L, Costello F, Albrecht P, Balcer L, Calabresi P, Frederiksen J, Frohman E, Green A, Klistorner A, Outteryck O, Paul F, Plant G, Traber G, Vermersch P, Villoslada P, Wolf S, Petzold A. Quality control for retinal OCT in multiple sclerosis: validation of the OSCAR-IB criteria. Mult Scler J. 2015 Feb 16;21(2):163–70.

34.   Smith SM, Zhang Y, Jenkinson M, Chen J, Matthews PM, Federico A, De Stefano N. Accurate, robust, and automated longitudinal and cross-sectional brain change analysis. Neuroimage. 2002 Sep;17(1):479–89.

35.   Tohka J. Partial volume effect modeling for segmentation and tissue classification of brain magnetic resonance images: A review. World J Radiol. 2014;6(11):855.

36.   Noval S, Contreras I, Muñoz S, Oreja-Guevara C, Manzano B, Rebolleda G. Optical coherence tomography in multiple sclerosis and neuromyelitis optica: an update. Mult Scler Int. 2011;2011:472790.

37.   Chien C, Juenger V, Scheel M, Brandt AU, Paul F. Considerations for Mean Upper Cervical Cord Area Implementation in a Longitudinal MRI Setting: Methods, Interrater Reliability, and MRI Quality Control. Am J Neuroradiol. 2020 Jan 23;

38.   Kuchling J, Backner Y, Oertel FC, Raz N, Bellmann-Strobl J, Ruprecht K, Paul F, Levin N, Brandt AU, Scheel M. Comparison of probabilistic tractography and tract-based spatial statistics for assessing optic radiation damage in patients with autoimmune inflammatory disorders of the central nervous system. NeuroImage Clin. 2018;19:538–50.

39. Hor JY, Asgari N, Nakashima I, Broadley SA, Leite MI, Kissani N, Jacob A, Marignier R, Weinshenker BG, Paul F, Pittock SJ, Palace J, Wingerchuk DM, Behne JM, Yeaman MR, Fujihara K. Epidemiology of Neuromyelitis Optica Spectrum Disorder and Its Prevalence and Incidence Worldwide. Vol. 11, Frontiers in Neurology. Frontiers Media S.A.; 2020.

40. Gold SM, Willing A, Leypoldt F, Paul F, Friese MA. Sex differences in autoimmune disorders of the central nervous system. Semin Immunopathol. 2019 Mar 25;41(2):177–88.

Statutory Declaration

"I, *Valentin, Jünger*, by personally signing this document in lieu of an oath, hereby affirm that I prepared the submitted dissertation on the topic *Evaluation of Optic Pathway Degeneration via Optic Chiasm Assessment in conventional MRI*, *Beurteilung der Degeneration der optischen Bahn via Chiasma Opticum Messung im konventionellen MRT*, independently and without the support of third parties, and that I used no other sources and aids than those stated. All parts which are based on the publications or presentations of other authors, either in letter or in spirit, are specified as such in accordance with the citing guidelines. The sections on methodology (in particular regarding practical work, laboratory regulations, statistical processing) and results (in particular regarding figures, charts and tables) are exclusively my responsibility.

Furthermore, I declare that I have correctly marked all of the data, the analyses, and the conclusions generated from data obtained in collaboration with other persons, and that I have correctly marked my own contribution and the contributions of other persons (cf. declaration of contribution). I have correctly marked all texts or parts of texts that were generated in collaboration with other persons.

My contributions to any publications to this dissertation correspond to those stated in the below joint declaration made together with the supervisor. All publications created within the scope of the dissertation comply with the guidelines of the ICMJE (International Committee of Medical Journal Editors; www.icmje.org) on authorship. In addition, I declare that I shall comply with the regulations of Charité – Universitätsmedizin Berlin on ensuring good scientific practice.

I declare that I have not yet submitted this dissertation in identical or similar form to another Faculty.

The significance of this statutory declaration and the consequences of a false statutory declaration under criminal law (Sections 156, 161 of the German Criminal Code) are known to me."

Date   Signature

Declaration of own contribution to the publications

Valentin Jünger contributed the following to the below listed publications:

Publication 1: Juenger V, Cooper G, Chien C, Chikermane M, Oertel FC, Zimmermann H, Ruprecht K, Jarius S, Siebert N, Kuchling J, Papadopoulou A, Asseyer S, Bellmann-Strobl J, Paul F, Brandt AU, Scheel M. Optic chiasm measurements may be useful markers of anterior optic pathway degeneration in neuromyelitis optica spectrum disorders. Eur Radiol. 2020 Apr 26;1–11.

Impact factor (2018): **3,962**
- Contribution in detail: Valentin Jünger conceived and designed this project, performed the MRI evaluation, the statistical analysis and data visualization. He was responsible for the data curation, methodology, software, validation and data interpretation. Specifically, Valentin Jünger wrote the original draft of the manuscript and all subsequent versions, reviewed and edited it for submission and publication. All tables (table 1 - 4) were created on the basis of his MRI analysis and statistical evaluation. Figures 3, 4 and 5 were created on the basis of the optic chiasm evaluation method he developed and used for MRI analysis. Figures 6, 7 and 8 were created on the basis of his statistical evaluation. Finally, he presented the project in a talk and a poster at the "MS Meeting 2019", a conference organized by the ARSEP foundation.

_____

Signature, date and stamp of first supervising university professor / lecturer

_____

Signature of doctoral candidate

Extract from the Journal Summary List s

Journal Data Filtered By: **Selected JCR Year: 2018** Selected Editions: SCIE,SSCI
Selected Categories: **"RADIOLOGY, NUCLEAR MEDICINE and MEDICAL IMAGING"** Selected Category Scheme: WoS
Gesamtanzahl: 129 Journale

Rank	Full Journal Title	Total Cites	Journal Impact Factor	Eigenfactor Score
1	JACC-Cardiovascular Imaging	8,801	10.975	0.026160
2	MEDICAL IMAGE ANALYSIS	7,694	8.880	0.013370
3	IEEE TRANSACTIONS ON MEDICAL IMAGING	19,545	7.816	0.024990
4	RADIOLOGY	54,641	7.608	0.061300
5	JOURNAL OF NUCLEAR MEDICINE	27,551	7.354	0.037990
6	EUROPEAN JOURNAL OF NUCLEAR MEDICINE AND MOLECULAR IMAGING	15,406	7.182	0.024760
7	CLINICAL NUCLEAR MEDICINE	4,922	6.498	0.007680
8	INTERNATIONAL JOURNAL OF RADIATION ONCOLOGY BIOLOGY PHYSICS	45,833	6.203	0.046810
9	INVESTIGATIVE RADIOLOGY	6,563	6.091	0.011150
10	Circulation-Cardiovascular Imaging	5,456	5.813	0.018480
11	NEUROIMAGE	99,720	5.812	0.132720
12	ULTRASOUND IN OBSTETRICS & GYNECOLOGY	12,336	5.595	0.020140
13	European Heart Journal-Cardiovascular Imaging	5,498	5.260	0.021650
14	RADIOTHERAPY AND ONCOLOGY	17,873	5.252	0.027470
15	Photoacoustics	512	5.250	0.001330
16	JOURNAL OF CARDIOVASCULAR MAGNETIC RESONANCE	5,113	5.070	0.014020
17	ULTRASCHALL IN DER MEDIZIN	2,238	4.613	0.003700
18	HUMAN BRAIN MAPPING	22,040	4.554	0.043230
19	JOURNAL OF NUCLEAR CARDIOLOGY	3,711	4.112	0.004480
20	EUROPEAN RADIOLOGY	19,597	3.962	0.033870

Print version of the included publication

NEURO

Optic chiasm measurements may be useful markers of anterior optic pathway degeneration in neuromyelitis optica spectrum disorders

Valentin Juenger [1,2,3] · Graham Cooper [1,2,4,5] · Claudia Chien [1,2] · Meera Chikermane [1,2] · Frederike Cosima Oertel [1,2,6] ·
Hanna Zimmermann [1,2] · Klemens Ruprecht [7] · Sven Jarius [8] · Nadja Siebert [2] · Joseph Kuchling [2,7] ·
Athina Papadopoulou [2,9] · Susanna Asseyer [2,7] · Judith Bellmann-Strobl [1,2] · Friedemann Paul [1,2,4,7] ·
Alexander U. Brandt [2,10] · Michael Scheel [2,3]

Abstract

Objectives We aimed to evaluate optic chiasm (OC) measures as potential imaging marker for anterior optic pathway damage assessment in the context of neuromyelitis optica spectrum disorders (NMOSD).

Materials and method This cross-sectional study included 39 patients exclusively with aquaporin 4-IgG seropositive NMOSD of which 25 patients had a history of optic neuritis (NMOSD-ON) and 37 age- and sex-matched healthy controls (HC). OC heights, width, and area were measured using standard 3D T1-weighted MRI. Sensitivity of these measures to detect neurodegeneration in the anterior optic pathway was assessed in receiver operating characteristics analyses. Correlation coefficients were used to assess associations with structural measures of the anterior optic pathway (optic nerve dimensions, retinal ganglion cell loss) and clinical measures (visual function and disease duration).

Results OC heights and area were significantly smaller in NMOSD-ON compared to HC (NMOSD-ON vs. HC $p < 0.0001$). An OC area *smaller than* 22.5 mm^2 yielded a sensitivity of 0.92 and a specificity of 0.92 in separating chiasms of NMOSD-ON from HC. OC area correlated well with structural and clinical measures in NMOSD-ON: optic nerve diameter ($r = 0.4$, $p = 0.047$), peripapillary retinal nerve fiber layer thickness ($r = 0.59$, $p = 0.003$), global visual acuity ($r = -0.57$, $p = 0.013$), and diseases duration ($r = -0.5$, $p = 0.012$).

Conclusion Our results suggest that OC measures are promising and easily accessible imaging markers for the assessment of anterior optic pathway damage.

Alexander U. Brandt and Michael Scheel contributed equally to this article.

✉ Friedemann Paul
  friedemann.paul@charite.de

1 Experimental and Clinical Research Center, Max Delbrueck Center for Molecular Medicine and Charité – Universitätsmedizin Berlin, corporate member of Freie Universität Berlin, Humboldt-Universität zu Berlin and Berlin Institute of Health, Berlin, Germany

2 NeuroCure Clinical Research Center, Charité – Universitätsmedizin Berlin, corporate member of Freie Universität Berlin, Humboldt-Universität zu Berlin and Berlin Institute of Health, Charitéplatz 1, 10117 Berlin, Germany

3 Department of Neuroradiology, Charité – Universitätsmedizin Berlin, corporate member of Freie Universität Berlin, Humboldt-Universität zu Berlin and Berlin Institute of Health, Berlin, Germany

4 Einstein Center for Neurosciences, Berlin, Germany

5 Department of Experimental Neurology and Center for Stroke Research Berlin, Charité – Universitätsmedizin Berlin, Berlin, Germany

6 Multiple Sclerosis Center, Dept. of Neurology, University of California San Francisco, San Francisco, CA, USA

7 Department of Neurology, Charité – Universitätsmedizin Berlin, corporate member of Freie Universität Berlin, Humboldt-Universität zu Berlin and Berlin Institute of Health, Berlin, Germany

8 Molecular Neuroimmunology Group, Department of Neurology, University of Heidelberg, Heidelberg, Germany

9 Neurologic Clinic and Policlinic, Departments of Medicine, Clinical Research and Biomedicine University Hospital Basel, Basel, Switzerland

10 Department of Neurology, University of California, Irvine, CA, USA

Springer

Key Points
• *Optic chiasm dimensions were smaller in neuromyelitis optica spectrum disorder patients compared to healthy controls.*
• *Optic chiasm dimensions are associated with retinal measures and visual dysfunction.*
• *The optic chiasm might be used as an easily accessible imaging marker of neurodegeneration in the anterior optic pathway with potential functional relevance.*

Keywords Optic neuritis · Optic chiasm · Magnetic resonance imaging · Neuromyelitis optica

Abbreviations

AQP4-IgG	Aquaporin 4-IgG
AUC	Area under the curve
CI	95% confidence interval
CoV	Coefficient of variation
EDSS	Expanded Disability Status Scale
GCIPL	Combined ganglion cell-inner plexiform layer
HC	Healthy controls
ICC	Intraclass correlations
logMAR	Logarithm of the minimum angle of resolution
NMOSD	Neuromyelitis optica spectrum disorders
NMOSD-ON	Neuromyelitis optica patients with history of optic neuritis
NMOSD-NON	Neuromyelitis optica patients without history of optic neuritis
OC	Optic chiasm
OCT	Optical coherence tomography
ON	Optic neuritis
pRNFL	Peripapillary retinal nerve fiber layer
ROC	Receiver operating characteristics

Introduction

Neuromyelitis optic spectrum disorders (NMOSDs) are inflammatory autoimmune CNS diseases that preferentially target the optic nerves and are frequently associated with serum autoantibodies to aquaporin-4 [1, 2]. Optic pathway degeneration following optic neuritis (ON) [3, 4] results in atrophy involving the entire visual pathway [5–10]. At the optic chiasma (OC), fibers from the left and the right optic nerve merge and form the site of highest axonal density. Direct damage or other pathophysiological effects affecting the optic nerves may accumulate in the OC, making it a promising target for the assessment of anterior optic pathway damage.

Measures of optic pathway degeneration are an important outcome measure of ON, since they are related to impaired visual function and reduction of vision-related quality of life [11–14]. Optic pathway dimensions as assessed by MRI have been used as a surrogate marker of inflammatory damage and atrophy of the optic nerve and anatomically connected tracts [3, 4, 15–18]. It has been suggested that MRI is sensitive to

axonal loss as a cause of optic nerve atrophy [17–20]. Optical coherence tomography (OCT) reveals damage to the retinal axons and ganglion cells by means of measuring peripapillary retinal nerve fiber layer (pRNFL) thickness and combined ganglion cell-inner plexiform layer (GCIPL) volume. OCT measures have been successfully used as surrogate markers of optic nerve atrophy [16, 17, 19, 21–25], being associated to MRI-detected macro- and microstructural optic pathway atrophy and visual function [16, 17, 20, 26–28].

Although MRI is used as part of the routine clinical workup of NMOSD patients [29, 30], no method to evaluate optic pathway damage has been established. In addition to the accumulation of damage within the anterior optic pathway, the OC appears particularly promising as a potential imaging marker, since it would simplify evaluation by reducing the region of interest from multiple structures to one. Only few studies have focused on the assessment of physiologic OC dimensions [31–33] and their changes in optic atrophy [18], while quantitative correlation analysis to visual function and optic pathway degeneration has not been performed.

The aim of this study was to assess whether neurodegenerative changes in the anterior optic pathway are detectable by assessing OC measures. We hypothesized that the OC assessment in standard 3D-T1w images is sensitive to anterior optic pathway damage. To test this hypothesis, we used NMOSD as a model for optic pathway damage and compared different OC measures (area, width, left, central, right, and total height) between aquaporin 4-IgG (AQP4-IgG) seropositive NMOSD patients with and without history of ON (NMOSD-ON and NMOSD-NON) and healthy controls (HC). In addition, we investigated the association of OC measures with optic nerve diameter, visual acuity, pRNFL thickness, and GCIPL volume in NMOSD-ON.

Material and methods

Study population

Data of 78 NMOSD patients acquired from an ongoing longitudinal prospective observational cohort study at the NeuroCure Clinical Research Center, Charité-Universitätsmedizin Berlin (recruited from May 2013 to January 2018) were screened for eligibility. All patients (i)

were 18 years or older and (ii) had a diagnosis of AQP4-IgG seropositive NMOSD according to the current panel criteria [29] and (iii) either had a last ON attack at least 5 months prior to MRI or had no history of ON. AQP4-IgG status was determined by a cell-based assay (Euroimmun, Lübeck, Germany). Patients with AQP4-IgG seronegative ($n = 25$) antibody status, unknown antibody status and/or incomplete clinical data ($n = 10$), lacking MRI data ($n = 3$), or ON within 5 months prior to MRI ($n = 1$) were excluded.

Thirty-nine patients exclusively with AQP4-IgG seropositive NMOSD and 37 age- and sex-matched HC subjects were included in this study (Table 1). All HC subjects were 18 years or older and had ophthalmologic testing and no history of neurological or ophthalmological diseases.

This study was approved by the local ethics committee (Ethikkommission der Charité–Universitätsmedizin Berlin; EA1/131/09) and conducted according the declaration of Helsinki and applicable German law. All participants gave written informed consent.

MRI acquisition

MRI data were acquired on the same 3-T scanner (MAGNETOM Trio, A Tim System, Siemens) at the Berlin Center for Advanced Neuroimaging using a volumetric high-resolution T1-weighted MPRAGE sequence (RT = 1900 ms, TE = 3.03 ms, TI = 900 ms, FOV = 256×256 mm^2, matrix 256×256, slice thickness 1 mm). OC measurements were performed on reconstructed 3D MPRAGE MR images.

Optic chiasm measures

After training with a neuroradiologist with more than 8 years of experience (M.S.), OC and optic nerve measurements were performed by V.J. (radiology trainee), blinded to clinical data, using a standardized protocol: First, the central point of the OC was determined on all 3 planes. The axes of the planes were reoriented to the course of the optic pathway, so that they were perpendicular to the orientation of the individual OC in the central point. On the individually reoriented transversal plane, OC area, heights, and width were measured. Optic nerve diameters were measured in the cisternal segment 7 mm anterior to the previously defined central point of the OC perpendicular to the optic nerve course (Figs. 1 and 2). All measurements were performed using region-of-interest software from Horos, version 3.3.2 (https://www.horosproject.org). Width was defined as the diameter along the adjusted frontal axis. Heights were measured perpendicularly to that diameter: central height at the middle, the lateral heights at the maximal diameter left and right to the center. For interrater reliability analysis, J.V. and M.C. (trainee) measured OC dimensions within 10 randomly selected HC and intraclass correlations (ICC) were calculated.

Clinical assessment

Neurological disability was on the Expanded Disability Status Scale (EDSS), including the visual functional system score according to the Neurostatus definitions [34]. Raters were

Table 1 Demographics and clinical characteristics

	HC	NMOSD-NON	NMOSD-ON	p
Number	37	14	25	–
Age, years (mean, SD)	47.8 (12.6)	53.8 (12.5)	48.09 (14.9)	0.33
Sex (F/M) (% female)	30/7 (81%)	14/0 (100%)	21/4 (84%)	0.22
Disease duration, years (median, range)	–	–	7.1 (3–34.1)	
Number of ON (median, range)	–	–	2 (1–12)	–
Time since first ON, years (median, range)	–	–	6.9 (3.4–32.2)	–
Time since last ON, years (median, range)	–	–	4.9 (0.5–13.2)	–
ON involvement, bilateral/unilateral	–	–	11/14 (8 right/6 left)	–
Optic nerve diameter, mm (mean, SD)	8.37 (0.50)	8.13 (0.90)	7.06 (1.23)	< 0.001
pRNFL, μm (mean, SD)	91.99 (15.10)	97.96 (10.13)	67.57 (17.92)	< 0.001
GCIPL mm^3 (mean, SD)	1.83 (0.28)	1.88 (0.14)	1.49 (0.25)	< 0.001
Visual acuity, logMAR (mean, SD)	− 0.01 (0.21)	−0.15 (0.21)	0.30 (0.63)	0.04
Visual Functional System Score (median, range)	–	0 (0–2)	1 (0–6)	< 0.001
EDSS (median, range)	–	3 (1–7)	4 (0–6.5)	0.71

p values are groupwise comparisons. *HC* = healthy controls; *NMOSD-ON* = neuromyelitis optica patients with history of optic neuritis; *NMOSD-NON* = neuromyelitis optica patients without history of optic neuritis; *ON* = optic neuritis; *pRNFL* = peripapillary retinal nerve fiber layer; *GCIPL* = combined ganglion cell-inner plexiform layer; *logMAR* = logarithm of the minimum angle of resolution; *EDSS* = Expanded Disability Status Scale
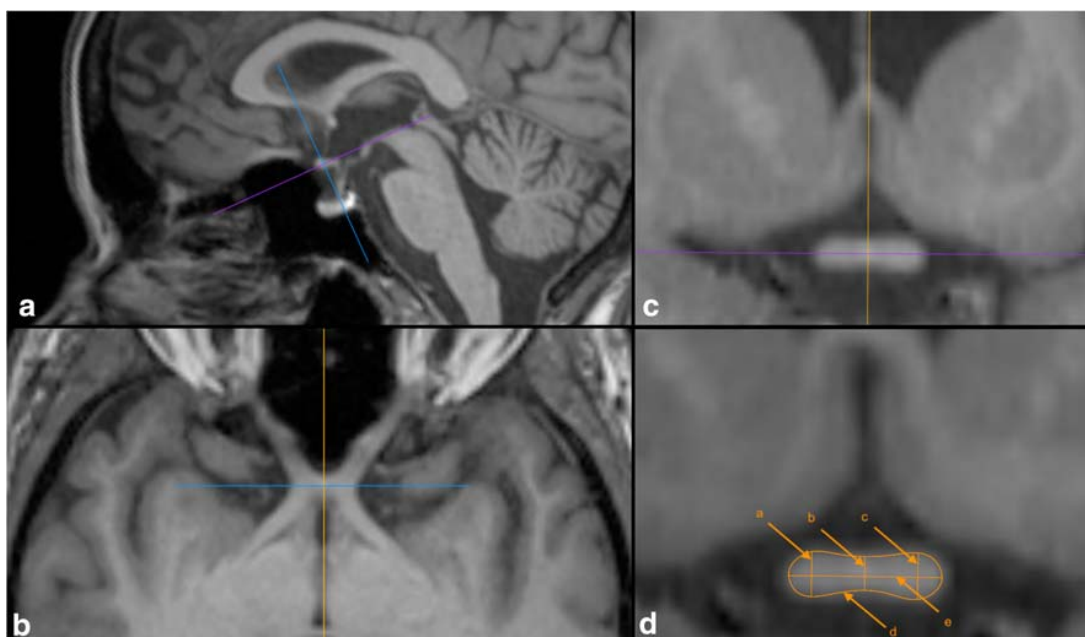
Fig. 1 Optic chiasm measurement. Panels **a**, **b**, and **c** illustrate how axes were adjusted perpendicularly to the orientation of the OC in the center point. Panel **d** shows a sample OC measurement (a = right, b = central, c = left height, d = area, e = width)

under the supervision of board-certified neurologists. The global neurological examination also included assessment of ON history using clinical criteria. Visual acuity was tested monocularly under phototopic conditions using retroilluminated Early Treatment in Diabetes Retinopathy Study charts at a 4-m distance. The logarithm of the minimum angle of resolution (logMAR) served as a measure of visual function. Visual acuity data was included only from patients where best correction was used ($n = 30$).

Optical coherence tomography measures

All OCT data were acquired on a spectral domain OCT device (Spectralis, Heidelberg Engineering) with automated real-time function. No pupil dilatation was used. We report the OCT acquisition settings and scanning protocol according to the APOSTEL recommendations [35]: The pRNFL thickness was measured using 3.4-mm ring scans around the optic nerve head (12°, 1536 A-scans, $9 \leq ART \leq 100$). The GCIPL volume was measured using a 6-mm diameter cylinder around the fovea from a macular volume scan (25°×30°, 61 vertical

B-scans, 768 A-scans per B-scan, ART = 15). Segmentation of the pRNFL and the intraretinal layers in the macular scan was performed semi-automatically using software provided by the optical coherence tomography manufacturer (Eye Explorer 1.9.10.0 with viewing module 6.0.9.0; Heidelberg Engineering). Quality was evaluated according to the OSCAR-IB criteria [36, 37].

Two patients did not have OCT data. Eight eyes from six NMOSD-ON had to be excluded due to incidental findings or quality reasons. Only the macular scan from two additional NMOSD-ON eyes was excluded due to quality reasons.

Statistics

Proportional group differences were tested with χ^2 test for sex and with ANOVA test for age. For comparison of ordinal and continuous measurements, groupwise comparison was performed using Kruskal-Wallis and ANOVA tests, respectively. Group comparison of OC dimensions was corrected for multiple comparison using the Holm-Bonferroni method. The variations of the individual metrics were compared within the HC
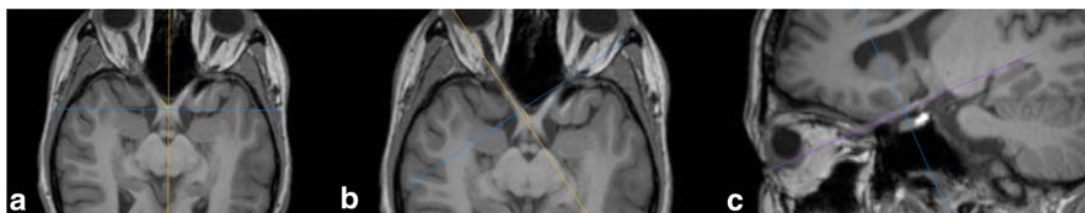

Fig. 2 Optic nerve measurement. Panels **a**, **b**, and **c** illustrate how axes were adjusted perpendicularly to the orientation of the optic nerve

group using a coefficient of variation (CoV) computed according to

$$CoV = \frac{standard\ deviation\ of\ the\ individual\ metric}{mean\ of\ the\ individual\ metric}$$

and served as an indicator of variation in the individual OC measures. Sensitivity to optic nerve atrophy of individual OC measures was evaluated with receiver operating characteristic (ROC) analysis, including area under the curve (AUC) comparison using DeLong method [38]. Association analysis of individual OC measures with the T2 lesion load, the SIENAX V-scaling [39] factor for head size and gender as potential influencing factors, mean optic nerve diameter, mean pRNFL thickness, mean GCIPL volume, visual function (mean logMAR), and disease duration was performed with the Pearson correlation test, association with the number of ON attacks with the Spearman test.

Statistical analyses were performed using R software, version 3.5.1. (http://www.r-project.org/) with the tidyverse [40], ggpubr [41], and pROC packages [42]. Statistical significance was set at a p value < 0.05.

Results

Demographics

Table 1 shows the demographic and clinical characteristics of the cohort. No significant differences of sex distribution, age, and physical disability were found between groups. Optic nerve diameters were different in NMOSD-ON compared to HC ($p < 0.0001$), NMOSD-ON compared to NMOSD-NON ($p < 0.01$), but not in NMOSD-NON compared to HC ($p > 0.05$).

Group comparison and receiver operating characteristics

Figure 3 shows the OC of NMOSD-ON, NMOSD-NON, and HC to illustrate the reduction of OC dimensions in NMOSD.

All OC measures except width were significantly smaller in all group comparisons (NMOSD-ON vs. HC: $p < 0.0001$; NMOSD-NON vs. HC: $p < 0.01$; and NMO-ON vs. NMO-NON: $p < 0.03$), as shown in Table 2 and Fig. 4. When correcting for multiple comparisons (corrected $p = 0.003$), this remained significant for all measures for HC vs. NMOSD-ON, for all measures except left height for HC vs. NMOSD-NON and for area for NMOSD-NON vs. NMOSD-ON.

OC measures were not associated with the T2 lesion load ($r = -0.35$, $p > 0.09$), the number of ON attacks ($r = -0.31$, $p > 0.13$), the number of ON attacks per side ($r = -0.09$,

$p > 0.13$), the SIENAX V-scaling factor, or gender ($r < 0.08$, $p > 0.23$). Thus, no correction for head size or sex was performed.

A ROC analysis was conducted to test the ability of the OC to predict the presence of damage in the anterior optic pathway, namely to differentiate between groups. OC area and OC heights have comparable AUC values for each group (NMOSD-ON vs. HC: AUC > 0.92; NMOSD-NON vs. HC: AUC > 0.74; NMO-ON vs. NMO-NON: AUC > 0.71), whereas width has lower AUC values, as shown in Table 3 and Fig. 5. AUC comparison using DeLong method and variation comparison using the CoV of the best performing measures revealed no significant difference. An OC area smaller than $22.5\ mm^2$ yielded a sensitivity of 0.92 and a specificity of 0.92 in separating chiasms of NMOSD-ON from HC.

Associations with structural and clinical measures

Table 4 summarizes the association analysis within the NMOSD-ON group. Higher OC measures were associated with bigger optic nerve diameter, better visual acuity, and better OCT measures. This was most prominent for OC area: Higher values significantly correlated with bigger optic nerve diameter ($r = 0.4$, $p = 0.047$), better logMAR ($r = -0.57$, $p = 0.013$), thicker pRNFL ($r = 0.59$, $p = 0.003$), bigger GCIPL ($r = 0.55$, $p = 0.007$), and shorter disease duration ($r = -0.5$, $p = 0.012$). Within OC heights, only central height was significantly associated with GCIPL ($r = 0.46$, $p = 0.028$).

Discussion

We evaluated OC measures as imaging marker of anterior optic pathway damage. We demonstrated significant group differences between NMOSD patients and HC and strong associations of OC measures with structural and clinical measures. Our data show that OC assessment in standard 3D-T1w images is sensitive to anterior optic pathway damage. Hence, OC measures are easily accessible and sensitive markers of anterior optic pathway damage.

OC dimension values for HC presented in our study are similar to recently published data [33]. A previous study by Wagner et al [31], however, reported slightly higher OC width and area values. This study excluded OC height due to a high degree of variance. Notably, unlike our study, Wagner et al did not account for the transverse course of the optic pathway and did not define precise measure locations. Thus, the coronal plane would be at varying angles (not perpendicular) to the course of the optic pathway at which OC assessment results in higher values and variance. Furthermore, our study employed a higher resolution MRI sequence, which may have an impact on values and variance.
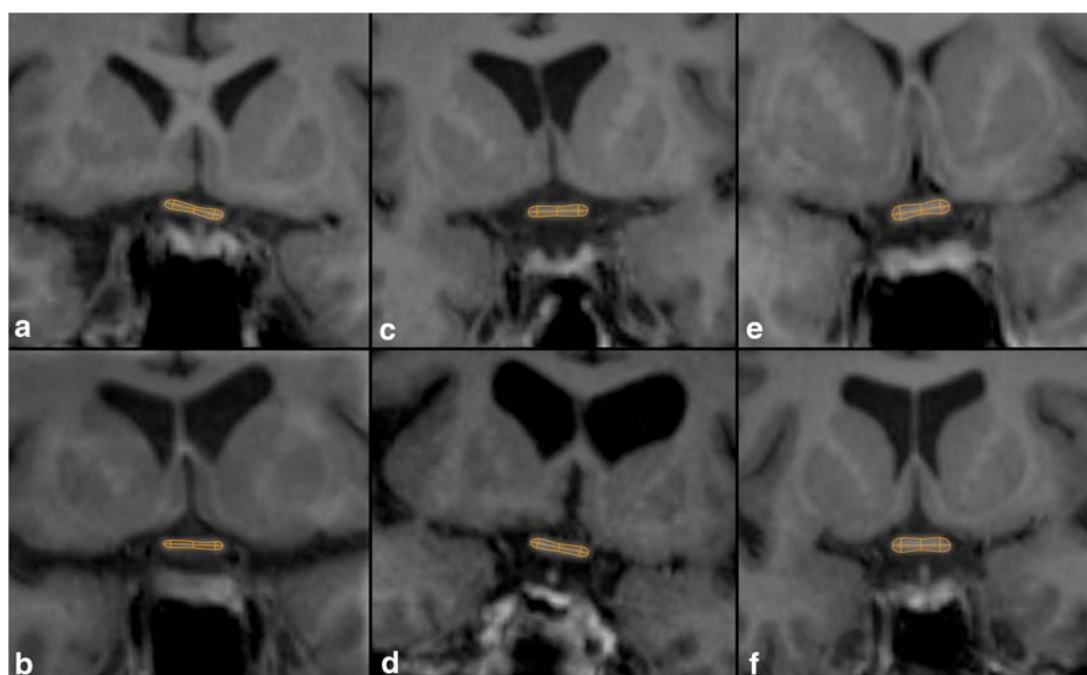
Fig. 3 Difference in optic chiasm dimensions. Shown are OCs of NMOSD-ON (**a**, **b**), NMOSD-NON (**c**, **d**), and HC (**e**, **f**)

OC heights and area showed differences between all groups. This is in line with earlier investigations suggesting that optic nerve dimensions discriminate ON patients from controls [16]. OC assessment, as suggested in our study, only requires a standard and broadly available MRI sequence (3D T1-weighted MPRAGE) and assesses a rather fixed structure less vulnerable to motion artifacts compared to the previously used orbital optic nerves [3, 4, 16, 17]. Note that in this study optic nerve diameters were measured in the cisternal segment 7 mm anterior to the OC, since contrast heterogeneity and motion artifacts in the orbital part rendered orbital assessment

difficult in 25% of the patients. The observation that smaller OC dimensions were also found in NMOSD-NON (compared to HC and NMOSD-ON) supports microstructural changes in the optic pathway independent of ON [26], which have been described in NMOSD [5, 27, 43, 44]. In concordance with a study by Harrigan et al [16], the optic nerve diameter was smaller in patients with a history of ON compared to HC but not in patients without ON. Although this should not be overstated in consideration of the small NMOSD-NON sample size, this might indicate that microstructural changes independent of ON, including anterograde degeneration

Table 2 Optic chiasm measures

Measure	HC	NMOSD-NON	NMOSD-ON	HC vs. NMOSD-NON	HC vs. NMOSD-ON	NMOSD-NON vs. NMOSD-ON	CoV	ICC
Left height (CI, mm)	2.77 (0.35)	2.34 (0.53)	1.94 (0.48)	$t = 2.77$ $p = 0.01$	$t = 7.49$ $p < 0.0001$	$t = 2.36$ $p = 0.03$	0.12	0.71
Central height (CI, mm)	1.93 (0.32)	1.55 (0.39)	1.22 (0.32)	$t = 3.27$ $p < 0.001$	$t = 8.63$ $p < 0.0001$	$t = 2.70$ $p = 0.013$	0.16	0.51
Right height (CI, mm)	2.65 (0.36)	2.20 (0.46)	1.79 (0.43)	$t = 3.31$ $p = 0.003$	$t = 8.23$ $p < 0.0001$	$t = 2.79$ $p = 0.008$	0.14	0.77
Width (CI, mm)	12.23 (1.15)	12.17 (1.05)	11.43 (1.87)	$t = 0.17$ $p = 0.56$	$t = 1.91$ $p = 0.059$	$t = 1.59$ $p = 0.18$	0.09	0.95
Area (CI, mm^2)	27.07 (3.50)	22.26 (4.65)	16.89 (4.44)	$t = 3.51$ $p = 0.003$	$t = 9.61$ $p < 0.0001$	$t = 3.51$ $p = 0.001$	0.13	0.89
Total height (CI, mm)	7.35 (0.90)	6.09 (1.33)	4.94 (1.14)	$t = 3.27$ $p = 0.003$	$t = 8.86$ $p < 0.0001$	$t = 2.73$ $p = 0.009$	0.12	0.76

Shown are means of OC measures. p and t-values are derived from t tests. Corrected $p = 0.003$. CI = 95% confidence interval; HC = healthy controls; $NMOSD$-ON = neuromyelitis optica patients with history of optic neuritis; $NMOSD$-NON = neuromyelitis optica patients without history of optic neuritis; CoV = coefficient of variation; ICC = intraclass correlations
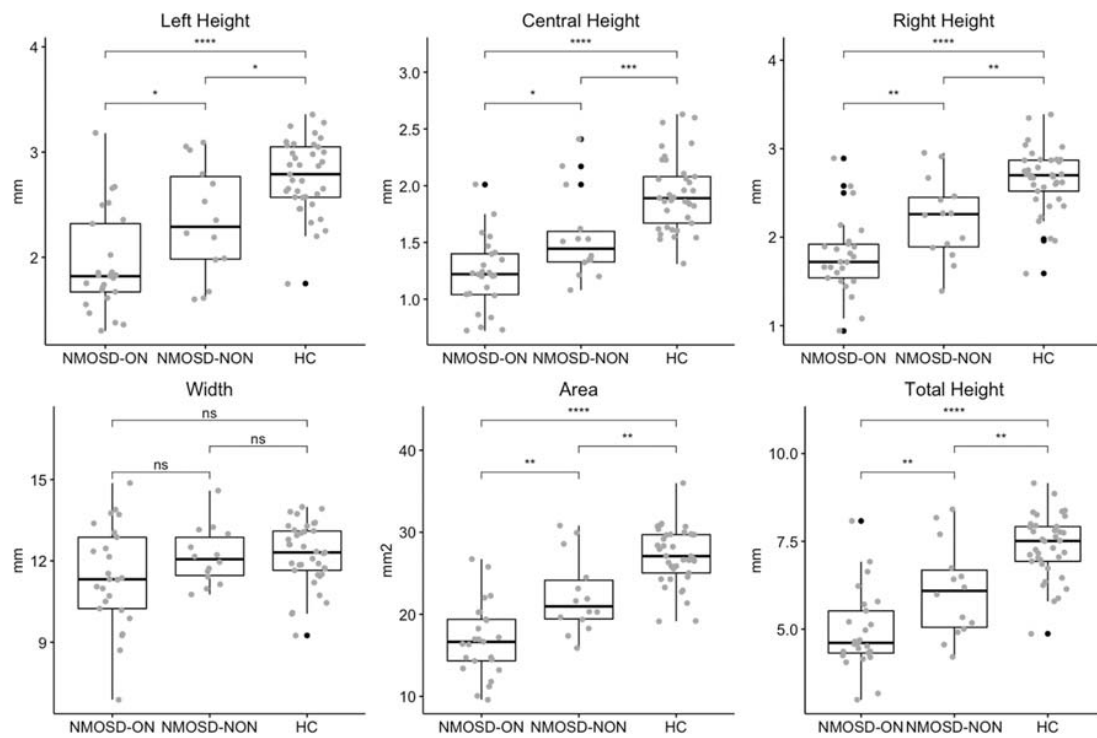
Fig. 4 Optic chiasm measures. Group differences in optic chiasm heights, width, and area between neuromyelitis optica spectrum disorders patients with optic neuritis (NMOSD-ON), without optic neuritis (NMOSD-NON), and healthy controls (HC). ns: $p > 0.05$, * $p \leq 0.05$, ** $p \leq 0.01$, *** $p \leq 0.001$, ****$p \leq 0.0001$

originating from anterior optic pathway damage but also retrograde degeneration originating from posterior optic pathway damage, might accumulate in the OC.

The AUC values obtained from ROC analyses for OC area and heights indicate that OC measures are sensitive to anterior optic pathway damage. On the descriptive level, OC left height shows slightly poorer ROC performance than right. This might rather be caused by an asymmetric severity of atrophy predominantly affecting fibers contributing to the right side of the OC (8 ON right vs. 6 ON left), of handedness

Table 3 Receiver operating characteristics analysis

HC vs. NMOSD-ON	Area	Width	Left Height	Central Height	Right Height	Total Height
AUC	0.95	0.64	0.90	0.95	0.92	0.94
95% CI	0.91–1.00	0.49–0.79	0.81–0.98	0.89–1.00	0.85–1.00	0.87–1.00
p value AUC comparison	–	< 0.01	0.02	0.78	0.16	0.40
HC vs. NMOSD-NON	**Area**	**Width**	**Left Height**	**Central Height**	**Right Height**	**Total Height**
AUC	0.78	0.55	0.74	0.80	0.78	0.77
95% CI	0.57–0.92	0.38–0.73	0.52–0.88	0.59–0.95	0.62–0.94	0.60–0.94
p value AUC comparison	–	0.08	0.31	0.49	0.93	0.77
NMOSD-ON vs. NMOSD-NON	**Area**	**Width**	**Left Height**	**Central Height**	**Right Height**	**Total Height**
AUC	0.81	0.63	0.71	0.74	0.76	0.76
95% CI	0.69–0.95	0.46–0.80	0.54–0.89	0.59–0.90	0.57–0.90	0.60–0.92
p value AUC comparison	–	0.08	0.06	0.19	0.29	0.14

Shown are area under the curve (AUC), 95% confidence interval (CI), and *p* value for AUC comparison using area as reference. *HC* = healthy controls; *NMOSD-ON* = neuromyelitis optica patients with history of optic neuritis; *NMOSD-NON* = neuromyelitis optica patients without history of optic neuritis
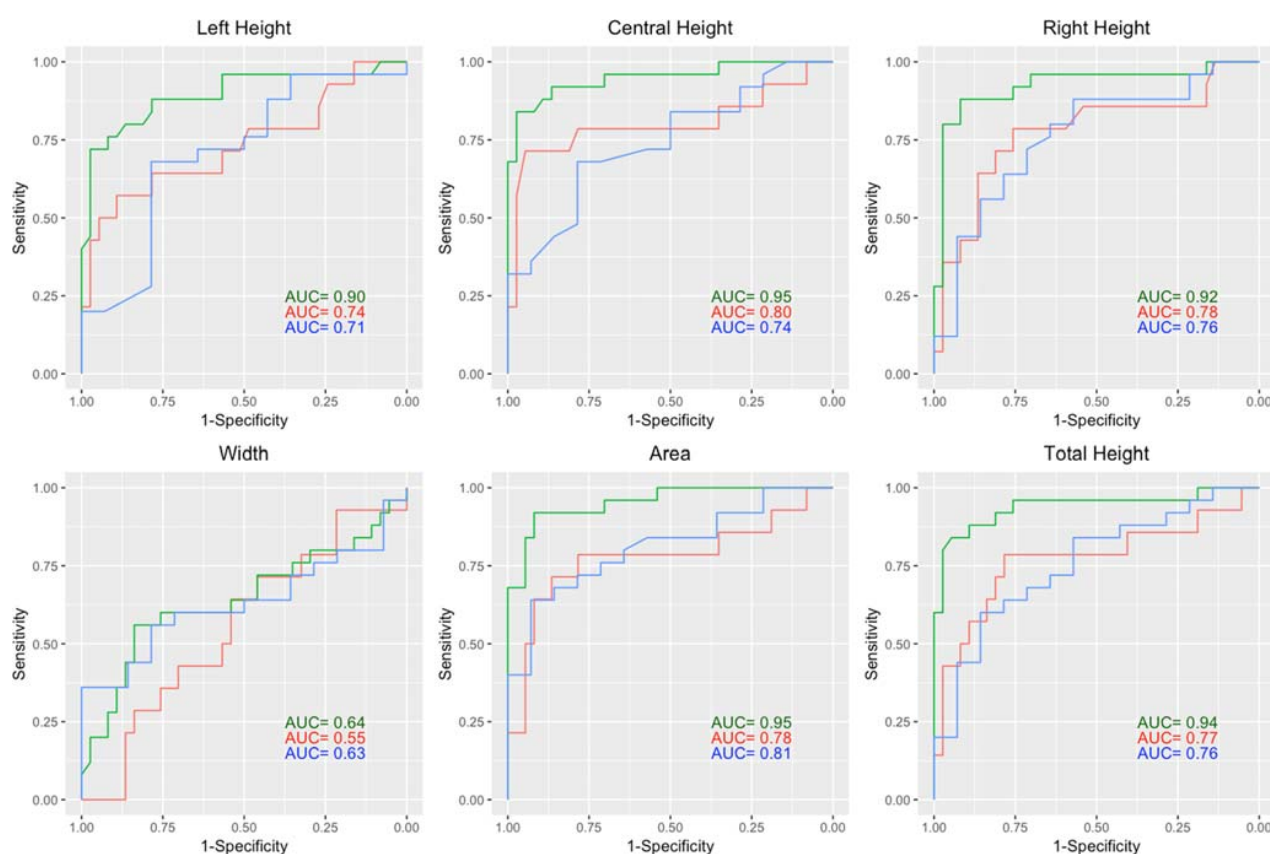
Fig. 5 Receiver operating characteristic for optic chiasm measures. Each line represents one group differentiation: green lines HC vs. NMOSD-ON, red lines HC vs. NMOSD-NON, blue lines NMOSD-ON vs. NMOSD-NON; ON = optic neuritis

or other asymmetries present in our study, than by a different sensitivity of the individual measure. This and the observation that no association between ON attacks per side and OC heights was found highlight the fact that OC assessment accumulates pathophysiologic processes of both sides and does not provide information on the origin of the fibers.

The observed associations between higher OC area and better visual acuity ($r = -0.57$), thicker pRNFL ($r = 0.53$) and bigger GCIPL ($r = 0.55$) in NMOSD are similar to the associations reported on optic nerve dimensions ($r = -0.50$, $r = 0.66$, $r = 0.59$) in MS [17]. The degree of association between pRNFL and anterior optic pathway dimensions in MRI

Table 4 Associations of OC measures and visual acuity, optic nerve diameter and optical coherence tomography measures for NMOSD-ON patients

Mean	Area	Width	Left Height	Central Height	Right Height	Total Height
Visual acuity (logMAR)	$r = -0.57$	$r = -0.53$	$r = -0.05$	$r = -0.43$	$r = -0.21$	$r = -0.22$
	$p = 0.013$	$p = 0.023$	$p = 0.84$	$p = 0.079$	$p = 0.41$	$p = 0.39$
Optic nerve diameter	$r = 0.4$	$r = 0.75$	$r = -0.06$	$r = -0.09$	$r = 0.09$	$r = -0.03$
	$p = 0.047$	$p < 0.001$	$p = 0.78$	$p = 0.68$	$p = 0.66$	$p = 0.87$
pRNFL thickness	$r = 0.59$	$r = 0.54$	$r = 0.15$	$r = 0.38$	$r = 0.30$	$r = 0.28$
	$p = 0.003$	$p = 0.008$	$p = 0.49$	$p = 0.07$	$p = 0.16$	$p = 0.19$
GCIPL volume	$r = 0.55$	$r = 0.33$	$r = 0.19$	$r = 0.46$	$r = 0.34$	$r = 0.33$
	$p = 0.007$	$p = 0.13$	$p = 0.39$	$p = 0.028$	$p = 0.11$	$p = 0.12$

r values are Pearson's correlation coefficients. *NMOSD-ON* = neuromyelitis optica patients with history of optic neuritis; *logMAR* = logarithm of the minimum angle of resolution; *pRNFL* = peripapillary retinal nerve fiber layer; *GCIPL* = combined ganglion cell-inner plexiform layer

might be equally limited in NMOSD and MS, since axonal loss is not the only substrate of neuronal atrophy and myelin loss, gliosis, and changes in water content also contribute to MRI-detected changes after ON [45]. Alongside findings suggesting that axonal loss is a major substrate of MRI-detected optic pathway atrophy after ON [17–20], the association between pRNFL (a surrogate for retinal axons) and OC measures implies that they are sensitive to atrophic changes of the anterior optic pathway. The association of OC area with visual function suggests a role for the OC as an imaging marker of neurodegenerative damage in the optic pathway with potential functional relevance.

Despite MRI's broad availability, no standardized MRI method for evaluation of optic pathway degeneration in standard scans is available. One major problem in optic nerve assessment is defining standardized measurement locations along the variable course of the nerve, which has high interindividual variability even in healthy populations [3, 4, 15, 17]. Several methods to measure optic nerve dimensions have been put forward [16, 17, 32]. These methods typically involve dedicated orbital MRI fat-saturated acquisition sequences along the axis of the optic nerve [3] additional to the commonly acquired sequences and extend the scan time for each patient. Others involve complex imaging postprocessing procedures [16] and, thus, may be difficult to implement in the routine clinical workup. Moreover, motion artifacts from eye movements and contrast reduction in the posterior region of the optic nerve, due to thinning of the CSF filled sub-arachnoid space, render MRI-based optic nerve assessment technically difficult [16]. This limits the accessibility of optic nerve measurements using MRI in the clinical setting.

The OC is less vulnerable to motion artifacts and consistently surrounded by CSF. It is less variable in morphology, bigger in dimensions and, thus, a simple target for MR investigations. OC assessment, as suggested in our study, only requires a broadly available MRI sequence (3D T1-weighted). While it does not provide information on the origin of the fibers and evaluation of focal optic nerve damage might better be achieved by direct measurement at the sight of inflammation, it accumulates neurodegeneration from both sides of the anterior optic pathway causing observable impairment. Thus, it extends the amount of information from a single measurement in the conventional and clinical standard scan, which can be used for monitoring of disease progression or therapeutic effectiveness.

Despite the low total number of subjects included in the study owing to the low prevalence of the disease, a significant difference in OC measures was shown within a relatively large homogeneous cohort exclusively consisting of AQP4-IgG-positive NMOSD patients. Separate gender analysis could not be conducted due to the high proportion of female patients. This is in line with the strong female preponderance in NMOSD [46]. OC width was measured along straight lines, which may not account for curved width. In future investigations, curved lines could be drawn; however, only few participants showed recognizable deviation from straight lines and, thus, we do not expect that this would drastically change the presented results.

Our data provide a strong rationale for future, larger studies on OC measures in ON, including in NMOSD patients with acute ON, in which inflammation might result in an increase in OC dimensions, as well as in patients with inflammatory diseases such as MS and myelin oligodendrocyte glycoprotein antibody associated disease (MOGAD) [47]. Finally, studies on the influence of susceptibility artifacts on scanners with different field strength and resolution seem justified and the application of advanced quantitative imaging methods such as DTI could reveal insights into the relationship between anterior and posterior optic pathway neurodegeneration.

Conclusion

Our study represents an initial and thorough assessment of OC measures to evaluate optic pathway degeneration using standard MRI and shows that the OC area is suitable and reliable. This simple method extends the amount of information that can be obtained from conventional and clinically available scans. Our results suggest that the OC might evolve into an easily accessible imaging marker of neurodegeneration in the anterior optic pathway with potential functional relevance.

Compliance with ethical standards

Guarantor The scientific guarantor of this publication is Friedemann Paul.

Conflict of interest The authors of this manuscript declare relationships with the following companies:

NS has received travel grants from Biogen Idec and sanofi-aventis/Genzyme.

SA received travel grants from Celgene GmbH, unrelated to this project.

FCO was employed by Nocturne, unrelated to this project.

HZ received research grants from Novartis, unrelated to this project.

KR was supported by the German Ministry of Education and Research (BMBF/KKNMS, Competence Network Multiple Sclerosis) and has received research support from Novartis and Merck Serono as well as speaking fees and travel grants from Guthy Jackson Charitable Foundation, Bayer Healthcare, Biogen Idec, Merck Serono, sanofi-aventis/Genzyme, Teva Pharmaceuticals, Roche, and Novartis.

JBS has received travel grants and speaking fees from Bayer Healthcare, Biogen Idec, Merck Serono, sanofi-aventis/Genzyme, Teva Pharmaceuticals, and Novartis.

FP declares that he has received research grants and speaker's honoraria from Bayer Healthcare, Teva Pharmaceuticals, Genzyme, Merck and Co., Novartis, and MedImmune. He is also a member of the steering committee for the OCTIMS study (run by Novartis).

AUB is cofounder and shareholder of technology start-ups Motognosis and Nocturne. He is named as inventor on several patent applications describing MS serum biomarkers, perceptive visual computing for motor function assessment and retinal image analysis.

Statistics and biometry   No complex statistical methods were necessary for this paper.

Informed consent   Written informed consent was obtained from all subjects (patients) in this study.

Ethical approval   Institutional Review Board approval was obtained.

Study subjects or cohorts overlap   Some study subjects or cohorts have been previously reported in PMID 31127016.

Methodology
• Retrospective
• Observational
• Performed at one institution

References

1. Jarius S, Wildemann B, Paul F (2014) Neuromyelitis optica: clinical features, immunopathogenesis and treatment. Clin Exp Immunol 176(2):149–164

2. Waters P, Reindl M, Saiz A et al (2016) Multicentre comparison of a diagnostic assay: aquaporin-4 antibodies in neuromyelitis optica. J Neurol Neurosurg Psychiatry 87(9):1005–1015

3. Hickman SJ, Brex PA, Brierley CM et al (2001) Detection of optic nerve atrophy following a single episode of unilateral optic neuritis by MRI using a fat-saturated short-echo fast FLAIR sequence. Neuroradiology 43:123–128

4. Hickman SJ, Toosy AT, Jones SJ et al (2004) A serial MRI study following optic nerve mean area in acute optic neuritis. Brain 127: 2498–2505

5. Tian DC, Su L, Fan M et al (2018) Bidirectional degeneration in the visual pathway in neuromyelitis optica spectrum disorder (NMOSD). Mult Scler 24:1585–1593

6. Tur C, Goodkin O, Altmann DR et al (2016) Longitudinal evidence for anterograde trans-synaptic degeneration after optic neuritis. Brain 139:816–828

7. Gabilondo I, Martinez-Lapiscina EH, Martinez-Heras E et al (2014) Trans-synaptic axonal degeneration in the visual pathway in multiple sclerosis. Ann Neurol 75:98–107

8. Sinnecker T, Oberwahrenbrock T, Metz I et al (2015) Optic radiation damage in multiple sclerosis is associated with visual dysfunction and retinal thinning~an ultrahigh-field MR pilot study. Eur Radiol 25:122–131

9. Kuchling J, Backner Y, Oertel FC et al (2018) Comparison of probabilistic tractography and tract-based spatial statistics for assessing optic radiation damage in patients with autoimmune inflammatory disorders of the central nervous system. Neuroimage Clin 19:538–550

10. Kuchling J, Brandt AU, Paul F, Scheel M (2017) Diffusion tensor imaging for multilevel assessment of the visual pathway: possibilities for personalized outcome prediction in autoimmune disorders of the central nervous system. EPMA J 8:279–294

11. Merle H, Olindo S, Bonnan M et al (2007) Natural history of the visual impairment of relapsing neuromyelitis optica. Ophthalmology 114:810–815

12. Schmidt F, Zimmermann H, Mikolajczak J et al (2017) Severe structural and functional visual system damage leads to profound loss of vision-related quality of life in patients with neuromyelitis optica spectrum disorders. Mult Scler Relat Disord 11:45–50

13. Stiebel-Kalish H, Hellmann MA, Mimouni M et al (2019) Does time equal vision in the acute treatment of a cohort of AQP4 and MOG optic neuritis? Neurol Neuroimmunol Neuroinflamm 6:e572

14. Beekman J, Keisler A, Pedraza O et al (2019) Neuromyelitis optica spectrum disorder: patient experience and quality of life. Neurol Neuroimmunol Neuroinflamm 6:e580

15. Hickman SJ, Brierley CM, Brex PA et al (2002) Continuing optic nerve atrophy following optic neuritis: a serial MRI study. Mult Scler 8:339–342

16. Harrigan RL, Smith AK, Lyttle B et al (2017) Quantitative characterization of optic nerve atrophy in patients with multiple sclerosis. Mult Scler J Exp Transl Clin 3:2055217317730097

17. Trip SA, Schlottmann PG, Jones SJ et al (2006) Optic nerve atrophy and retinal nerve fibre layer thinning following optic neuritis: evidence that axonal loss is a substrate of MRI-detected atrophy. Neuroimage. 31:286–293

18. Parravano JG, Toledo A, Kucharczyk W (1993) Dimensions of the optic nerves, chiasm, and tracts: MR quantitative comparison between patients with optic atrophy and normals. J Comput Assist Tomogr 17:688–690

19. Manogaran P, Vavasour IM, Lange AP et al (2016) Quantifying visual pathway axonal and myelin loss in multiple sclerosis and neuromyelitis optica. Neuroimage Clin 11:743–750

20. Manogaran P, Hanson JV, Olbert ED et al (2016) Optical coherence tomography and magnetic resonance imaging in multiple sclerosis and Neuromyelitis Optica Spectrum disorder. Int J Mol Sci 17: e1894

21. Trip SA, Schlottmann PG, Jones SJ et al (2005) Retinal nerve fiber layer axonal loss and visual dysfunction in optic neuritis. Ann Neurol 58:383–391

22. Oertel FC, Zimmermann HG, Brandt AU, Paul F (2018) Novel uses of retinal imaging with optical coherence tomography in multiple sclerosis. Expert Rev Neurother 19:31–43

23. Oberwahrenbrock T, Traber GL, Lukas S et al (2018) Multicenter reliability of semiautomatic retinal layer segmentation using OCT. Neurol Neuroimmunol Neuroinflamm 5:e449

24. Dorr J, Wernecke KD, Bock M et al (2011) Association of retinal and macular damage with brain atrophy in multiple sclerosis. PLoS One 6:e18132

25. Ayadi N, Dörr J, Motamedi S (2018) Temporal visual resolution and disease severity in MS. Neurol Neuroimmunol Neuroinflamm 5(5):e49

26. Oertel FC, Zimmermann H, Paul F, Brandt AU (2018) Optical coherence tomography in neuromyelitis optica spectrum disorders: potential advantages for individualized monitoring of progression and therapy. EPMA J 9:21–33

27. Oertel FC, Kuchling J, Zimmermann H et al (2017) Microstructural visual system changes in AQP4-antibody-seropositive NMOSD. Neurol Neuroimmunol Neuroinflamm 4:e334

28. Bennett JL, de Seze J, Lana-Peixoto M et al (2015) Neuromyelitis optica and multiple sclerosis: seeing differences through optical coherence tomography. Mult Scler 21:678–688

29. Wingerchuk DM, Banwell B, Bennett JL et al (2015) International consensus diagnostic criteria for neuromyelitis optica spectrum disorders. Neurology 85:177–189

30. Kim HJ, Paul F, Lana-Peixoto MA et al (2015) MRI characteristics of neuromyelitis optica spectrum disorder: an international update. Neurology 84:1165–1173

31. Wagner AL, Murtagh FR, Hazlett KS, Arrington JA (1997) Measurement of the normal optic chiasm on coronal MR images. AJNR Am J Neuroradiol 18:723–726

32. Avery RA, Mansoor A, Idrees R et al (2016) Quantitative MRI criteria for optic pathway enlargement in neurofibromatosis type 1. Neurology 86:2264–2270

33. Kasmann-Kellner B, Schafer T, Krick CM, Ruprecht KW, Reith W, Schmitz BL (2003) Anatomical differences in optic nerve, chiasma and tractus opticus in human albinism as demonstrated by standardized clinical and MRI evaluation. Klin Monbl Augenheilkd 220: 334–344

34. Kurtzke JF (1983) Rating neurologic impairment in multiple sclerosis. Neurology. 33:1444–1452

35. Cruz-Herranz A, Balk LJ, Oberwahrenbrock T et al (2016) The APOSTEL recommendations for reporting quantitative optical coherence tomography studies. Neurology 86:2303–2309

36. Tewarie P, Balk L, Costello F et al (2012) The OSCAR-IB consensus criteria for retinal OCT quality assessment. PLoS One 7:e34823

37. Schippling S, Balk L, Costello F et al (2015) Quality control for retinal OCT in multiple sclerosis: validation of the OSCAR-IB criteria. Mult Scler 21:163–170

38. Hajian-Tilaki K (2013) Receiver operating characteristic (ROC) curve analysis for medical diagnostic test evaluation. Caspian J Intern Med 4:627–635

39. Smith SM, ThangY JM et al (2002) Accurate, robust, and automated longitudinal and cross-sectional brain change analysis. Neuroimage 17:479–489

40. Wickham H (2017) Tidyverse: easily Install and Load the "Tidyverse.". Available via https://cranr-project.org/package. Accessed 10 Oct 2018

41. Kassambara A (2017) ggpubr: "ggplot2" Based Publication Ready Plots. Available via https://cran.r-project.org/web/packages/ggpubr/index.html. Accessed 10 Oct 10 2018

42. Robin X, Turck N, Hainard A et al (2011) pROC: an open-source package for R and S+ to analyze and compare ROC curves. BMC Bioinformatics 12:77

43. Akaishi T, Kaneko K, Himori N et al (2017) Subclinical retinal atrophy in the unaffected fellow eyes of multiple sclerosis and neuromyelitis optica. J Neuroimmunol 313:10–15

44. Oertel FC, Havla J, Roca-Fernandez A et al (2018) Retinal ganglion cell loss in neuromyelitis optica: a longitudinal study. J Neurol Neurosurg Psychiatry 89:1259–1265

45. Noval S, Contreras I, Muñoz S, Oreja-Guevara C, Manzano B, Rebolleda G (2011) Optical coherence tomography in multiple sclerosis and neuromyelitis optica: an update. Mult Scler Int 2011: 472790

46. Gold SM, Willing A, Leypoldt F, Paul F, Friese MA (2019) Sex differences in autoimmune disorders of the central nervous system. Semin Immunopathol 41:177–188

47. Borisow N, Mori M, Kuwabara S, Scheel M, Paul F (2018) Diagnosis and treatment of NMO spectrum disorder and MOG-encephalomyelitis. Front Neurol 9:888

Curriculum vitae

Mein Lebenslauf wird aus datenschutzrechtlichen Gründen in der elektronischen Version meiner Arbeit nicht veröffentlicht.

My curriculum vitae is not published in the electronic version of my dissertation for data protection reasons.

List of Publications

An up-to-date list is available here: https://orcid.org/0000-0002-8098-178X

Peer reviewed original research articles

Juenger V, Cooper G, Chien C, Chikermane M, Oertel FC, Zimmermann H, Ruprecht K, Jarius S, Siebert N, Kuchling J, Papadopoulou A, Asseyer S, Bellmann-Strobl J, Paul F, Brandt AU, Scheel M. Optic chiasm measurements may be useful markers of anterior optic pathway degeneration in neuromyelitis optica spectrum disorders. Eur Radiol. 2020 Apr 26;1–11.

Chien C, **Juenger V**, Scheel M, Brandt AU, Paul F. Considerations for Mean Upper Cervical Cord Area Implementation in a Longitudinal MRI Setting: Methods, Interrater Reliability, and MRI Quality Control. Am J Neuroradiol. 2020 Jan 23;41(2) 343-350.

Conference abstracts

V. Juenger, G. Cooper, C. Chien, et al. Optic Chiasm Assessment on clinical standard 3D T1w-MRI detects Optic Nerve Atrophy. *Multiple Sclerosis Meeting: 50 years of International research for ARSEP Foundation.* 2019. (Poster)

Cooper G, Chien C, **Juenger V**, Bellmann-Strobl J, Kuchling J, Asseyer S, Ruprecht K, Brandt AU, Scheel M, Paul F, Finke C. Association between humoral cerebrospinal fluid markers, periventricular lesion density and cortical thickness in early multiple sclerosis. ECTRIMS 2019 - Poster Session 1, 2019. *Multiple Sclerosis Journal*; 2019; 2: P533.

Chien C, **Juenger V**, Scheel M, Brandt AU, Paul F. Longitudinal variability of spinal cord atrophy as measured by the mean upper cervical cord area. ECTRIMS 2019 - Poster Session 1, 2019. *Multiple Sclerosis Journal.* 2019; 2: P523.

Acknowledgements